Spring 2-2015

The Development of Advanced Control Laboratories

Matthew Randall Winter
wintermr@rose-hulman.edu

The Development of Advanced Control Laboratories

A Thesis

Submitted to the Faculty

of

Rose-Hulman Institute of Technology

by

Matthew Randall Winter

In Partial Fulfillment of the Requirements for the Degree

of

Masters of Science in Mechanical Engineering

February 2015

ROSE-HULMAN INSTITUTE OF TECHNOLOGY

Final Examination Report

Matthew R. Winter	Mechanical Engineering
Name	Graduate Major

Thesis Title: The Development of Advanced Controls Laboratories

DATE OF EXAM: January 20, 2015

EXAMINATION COMMITTEE:

	Thesis Advisory Committee	Department
Thesis Advisor:	Dr. Bradley Burchett	ME
	Dr. Daniel Kawano	ME
	Dr. Ronald Artigue	CHE

PASSED X **FAILED** _____

ABSTRACT

Winter, Matthew Randall

M.S.M .E.

Rose-Hulman Institute of Technology

February 2015

The Development of Advanced Controls Laboratories

Thesis Advisor: Dr. Bradley Burchett

In this thesis, a series of advanced control labs have been developed for use in the senior/graduate-level advanced controls course. Advanced controls laboratories are non-existent at many institutions, and since hands on laboratories are such an integral part of engineering education it was decided to develop a few. The goal of these laboratories is to reinforce some of the more advanced topics in control theory. Topics of the laboratories include Parameter Identification, Eigenstructure Assignment, Linear Optimal Regulators and Linear Quadratic Gaussian Control with Loop Transfer Recovery. These laboratories are carried out on the Educational Control Products Model 210 Rectilinear Control System with the disturbance motor add on using MATLAB/Simulink Real Time Workshop with Real Time Windows Target.

Acknowledgements

I would like to express my appreciation to my advisor Dr. Bradley T. Burchett. Thank you for providing the opportunity to help advance controls education at Rose-Hulman. I would also like to thank Brianna Roux for her help with manipulating Microsoft Word.

TABLE OF CONTENTS

Contents

LIST OF FIGURES

Figure Page

LIST OF TABLES

Table Page

LIST OF ABBREVIATIONS

ECP	Educational Control Products
RTW	Real Time Window
RTWT	Real Time Window Target
ECP210	ECP Model 210 Rectilinear Control System
LQG	Linear Quadratic Gaussian
LTR	Loop Transfer Recovery
LQR	Linear Quadratic Regulator
CARE	Control Algebraic Riccati Equation
FARE	Filter Algebraic Riccati Equation
MIMO	Multi-Input Multi-Output
SISO	Single-Input Single-Output
DOF	Degree of Freedom

GLOSSARY

Eigenstructure Assignment — a procedure used to develop a linear gain matrix for feedback control so that the resulting system has a desirable closed-loop response.

Loop Transfer Recovery — a procedure that allows one to design a state feedback loop with desirable properties and then to asymptotically "recover" those properties using an appropriate choice of observer gains.

Linear Quadratic Gaussian — one of the most fundamental optimal control problems. It concerns an uncertain linear system disturbed by additive white Gaussian noise, having incomplete state information and undergoing control subject to quadratic costs.

Linear Quadratic Regulator — the optimal theory of pole placement method where the cost is described by a quadratic function.

Kalman Filter — an algorithm that uses a series of measurements observed over time, containing noise and other inaccuracies, and produces estimates of unknown variables that tend to be more precise than those based on a single measurement alone.

Algebraic Riccati Equation — a type of quadratic matrix equation that arises in the context of infinite-horizon optimal control problems in continuous time or discrete time. In such a problem, one cares about the value of some variable of interest arbitrarily far into the future, and one must optimally choose a value of a controlled variable right away, knowing that one will also behave optimally at all times in the future. The optimal current values of the problem's control variables at any time can be found using the solution of the Riccati equation and the current observations on evolving state variables. With multiple state variables and multiple control variables, the Riccati equation will be a matrix equation.

1. INTRODUCTION

1.1 Motivations

The function of engineers is to manipulate materials, energy and information for the benefit of mankind. In order to do this, engineers must gain knowledge in other ways than purely classroom learning [1]. In controls classes, the addition of laboratories is a valuable step to helping students understand control theory [2]. At many universities advanced control engineering laboratories are non-existent, instead being reduced to pure simulation owing in part to the relatively high cost of the former and the changing motivation of faculties away from contributions to undergraduate education and more towards research productivity [1, 3]. To this end it was deemed appropriate to conceive of several laboratories to demonstrate some of the more theoretical concepts in advanced control theory using existing equipment.

1.2 Historical Background

Hands-on control laboratories with hardware in the loop have been an important part of controls education since the introduction of analog computers at the University of Michigan's Department of Aeronautical Engineering in 1956 [4]. Since then, the use of the personal computer has streamlined some of the more tedious steps in analog simulation leading to the release of commercially available prepackaged experiments by 1992 from companies such as Educational Control Products (ECP) and Feedback Instruments [4, 5]. Today, at Rose-Hulman Institute of Technology, students use MATLAB / Simulink Real Time Workshop (RTW) with Real Time Windows Target (RTWT) in conjunction with the ECP Model 210 Rectilinear

Control System (ECP210) and the ECP Model 205 Torsional Control System to gain insight into the basics of control theory through laboratories.

1.3 Overview

A series of advanced control experiments have been developed for use in the senior/graduate level advanced controls course, ME506. The ECP210 with the disturbance motor add-on is used for these experiments. This plant is a precisely instrumented mechanical system that is configurable for a number of degrees of freedom and plant parameters. The ECP210 can be seen in Figure 1.1.

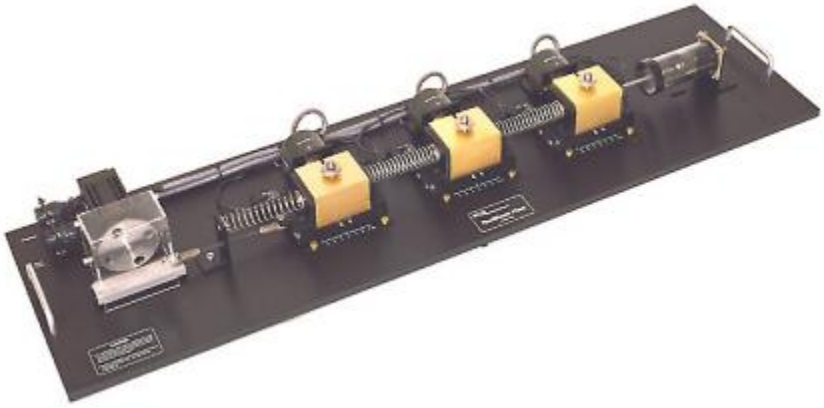

Figure 1.1:The ECP Rectilinear Control System (ECP 210) [6]

Chapter 2 describes the cart parameter identification procedure. Chapter 3 describes a laboratory using eigenstructure assignement to decouple a multi-input multi-output system. Chapter 4 describes a laboratory about the implementation of a finite horizon linear optimal regulator that will solve a simple single-input single-output optimal control problem. Chapter 5 describes a laboratory using the Linear Quadradic Gaussian with Loop Transfer Recovery to discuss how the Loop Transfer Recovery procedure produces better estimate of the states.

2. PARAMETER IDENTIFICATION

2.1 Experiment Goals

The main goal of this laboratory is to identify important system characteristics of both of the carts and motors using a step response and a frequency response approach. In order to obtain these characteristics, four trials of the physical model with varying mass are preformed and parameters such as damping ratio and natural frequency are calculated. A set of over determined equations is used to determine the carts' mass and spring constant. The hardware gains of the motors and the damping coefficients of the system are then solved by back substitution using a 5×5 upper triangular matrix. These values should then be utilized in a purely theoretical step response to see how they compare to the actual data obtained. Then the students should perform a frequency response of the second cart.

2.2 Experimental Procedure

The experiment uses the ECP210, shown in Figure 1.1, consisting of two single-degree-of-freedom mass-spring-damper systems. The mass is adjustable by adding or removing plates in increments of 500 grams. The masses were set in the carts where they were held down with a small screw so they would not move during the experiment. This test involved using three different added mass values of 1500 grams, 1000 grams, and 500 grams, as shown in Table 2.1, with the first cart attached on the left with a stiff spring and the second cart attached on the right with a light spring to the third cart which is fixed.

Table 2.1: Variable mass of Carts

Case#	Added Mass (g)	Cart 1 Spring	Cart 2 Spring
1	1500	stiff	light
2	1000	stiff	light
3	500	stiff	light
4	0	stiff	light

The Simulink RTW for the step response is shown in Figure 2.1 below.

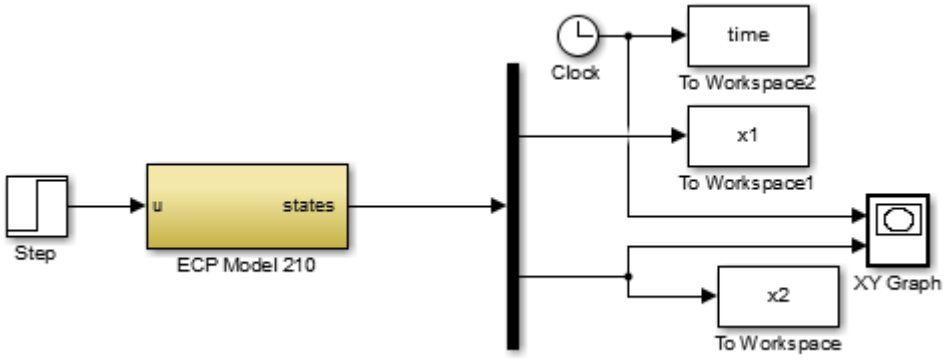

Figure 2.1: Simulink RTW step response

The frequency response should be conducted by running the trials in Table 2.2

Table 2.2: Frequency and Amplitude

Case	Amplitude	Frequency (Hz)	Added Mass (g)
1	0.02	3	500
2	0.03	4	500
3	0.02	5	500
4	0.04	6	500
5	0.06	7	500
6	0.01	8	500

The Simulink RTW for the frequency response is shown in Figure 2.2 below.

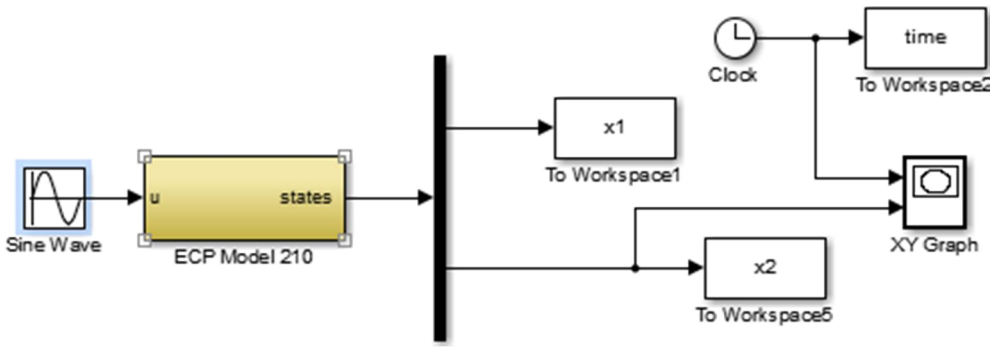

Figure 2.2: Simulink RTW frequency response

It is imperative that the amplitude not be too high or else the disturbance motor could potentially break. Students should use the findmag2 MATLAB function, attached in Appendix A, to find the magnitude of each response. The frequencies are to be converted into radians per second, after which the common logarithm should be taken. This is to be plotted against the magnitude in decibels and the intercept of the line of best fit shall be used to find the characteristic disturbance motor gain.

2.3 Method of Analysis

After all trials are complete, the data must be analyzed. In order to do so a basic method of parameter identification is used [7]. The idealized mass-spring-damper system can be seen in Figure 2.3.

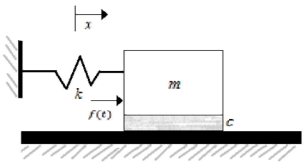

Figure 2.3: Idealized Mass-Spring-Damper Model

The equation of motion for a mass-spring-damper system is the following:

$$\frac{m}{k}\ddot{x} + \frac{c}{k}\dot{x} + x = \frac{f(t)}{k} \tag{2.1}$$

where *m* is the equivalent mass constant, *c* is the damping constant, *k* is the spring constant and *f(t)* is the force input. However, the force input is not what is transmitted directly to the hardware by Simulink. Instead, there is an unknown hardware gain that scales the step magnitude into a force input on the system as follows:

$$f(t) = C_{hw}g(t) \tag{2.2}$$

where C_{hw} is the unknown hardware gain and $g(t)$ is the Simulink input to the system. Substituting (2.2) into (2.1) gives:

$$\frac{m}{k}\ddot{x} + \frac{c}{k}\dot{x} + x = \frac{C_{hw}g(t)}{k} \tag{2.3}$$

However, these values cannot simply be read from the plots created from the data. Instead, a plot of the step response provides key information that can be extracted, such as peak response (x_{peak}), steady-state response (x_{ss}), peak time (t_p), and percent overshoot (po). A representative second-order step response plot with any given parameters and initial conditions equal to zero exhibits the performance measures as shown in Figure 2.4.

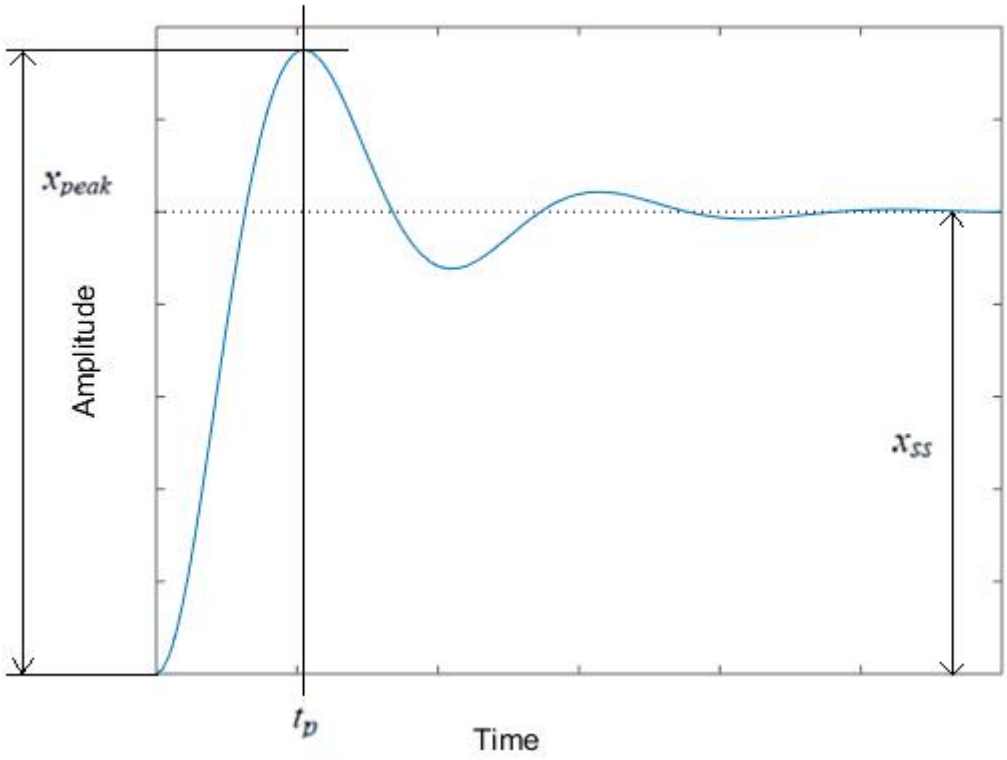

Figure 2.4: Representative Second Order Step Response

With only this information one cannot go directly from the given by the plot back to equation (2.3). Therefore we re-write (2.3) in standard form as follows:

$$\frac{1}{\omega_n^2}\ddot{x} + \frac{2\zeta}{\omega_n}\dot{x} + x = Kg(t) \tag{2.4}$$

Now we are trying to find the natural frequency (ω_n) of the system, the damping ratio (ζ) and *K,* the static gain, not to be confused with the spring constant, *k*. By finding the standard parameters, the system parameters can be found by matching coefficients with (2.3), which is the ultimate goal. To do so first solve for *K* using

$$K = \frac{x_{ss}}{u_0} \tag{2.5}$$

where $u_0$is the magnitude of the step input. Next, the damping ratio must be found, but in order to accomplish that we first need to find the percent overshoot of the system, po:

$$po = \frac{x_{peak} - x_{ss}}{x_{ss}} \tag{2.6}$$

Note that the values for x_{peak} and x_{ss} can easily be determined by referring back to graphs such as Figure 2.4. Now, ζ can be easily calculated using the value of po as follows:

$$\zeta = \sqrt{\frac{(\ln(po))^2}{\pi^2 + (\ln(po))^2}} \tag{2.7}$$

Two of the three parameters from (2.4) have been found but the natural frequency still needs to be determined. Doing so requires two steps. First, solve for the damped natural frequency, ω_d, using the peak time, t_p, from graphs such as Figure 2.4:

$$\omega_d = \frac{\pi}{t_p} \tag{2.8}$$

Finally ω_n can be solved for using the values determined in (2.7) and (2.8) as follows:

$$\omega_d = \omega_n\sqrt{1 - \zeta^2} \tag{2.9}$$

The previous calculations have resulted in finding the three necessary values from (2.4). However, the main goal of the lab is to find *m, c, k,* and C_{hw} for (2.3). Coefficient matching is now employed for this very purpose. The same procedure is to be followed for both carts from Table 2.1. Defining the natural frequency by comparing coefficients in (2.3) and (2.4) gives

$$\omega_{n,i} = \sqrt{\frac{k}{m_{ti}}} \tag{2.10}$$

where the subscript i indicates that four equations can be written, one for each case and m_{ti} is the total mass of the cart for each case which gives

$$m_{ti} = m_{eq,cart} + m_{added} \tag{2.11}$$

where $m_{eq,cart}$ is the equivalent mass of the cart and m_{added} is the amount of mass added to the cart as specified in Table 2.1. By combining (2.10) with the definition of the damped natural frequency from (2.9) we get

$$\omega_{d,i} = \sqrt{\frac{k}{m_{ti}}}\sqrt{1-\zeta_i^2} \tag{2.12}$$

Rearranging (2.12) for each case gives the following set of equations:

$$m_{t1}\omega_{d_1}^2 - k(1-\zeta_1^2) = 0 \tag{2.13}$$
$$m_{t2}\omega_{d_2}^2 - k(1-\zeta_2^2) = 0 \tag{2.14}$$
$$m_{t3}\omega_{d_3}^2 - k(1-\zeta_3^2) = 0 \tag{2.15}$$
$$m_{t4}\omega_{d_4}^2 - k(1-\zeta_4^2) = 0 \tag{2.16}$$

Now there are five unknowns, m_{ti} and k. However, three additional equations can be written based on the known difference in the added masses:

$$m_{t1} - m_{t2} = 0.5 \tag{2.17}$$
$$m_{t1} - m_{t3} = 1 \tag{2.18}$$
$$m_{t3} - m_{t4} = 0.5 \tag{2.19}$$

This gives an over-determined set of equations which can be solved using linear algebra. Rewriting (2.13)-(2.19) in matrix-vector form results in (2.20). We use (2.20) to solve for cart mass and stiffness.

$$\begin{bmatrix} \omega_{d_1}^2 & 0 & 0 & 0 & -(1-\zeta_1^2) \\ 0 & \omega_{d_2}^2 & 0 & 0 & -(1-\zeta_2^2) \\ 0 & 0 & \omega_{d_3}^2 & 0 & -(1-\zeta_3^2) \\ 0 & 0 & 0 & \omega_{d_4}^2 & -(1-\zeta_4^2) \\ 1 & -1 & 0 & 0 & 0 \\ 1 & 0 & -1 & 0 & 0 \\ 0 & 0 & 1 & -1 & 0 \end{bmatrix} \begin{Bmatrix} m_{t1} \\ m_{t2} \\ m_{t3} \\ m_{t4} \\ k \end{Bmatrix} = \begin{Bmatrix} 0 \\ 0 \\ 0 \\ 0 \\ 0.5 \\ 1.0 \\ 0.5 \end{Bmatrix} \tag{2.20}$$

Solving (2.20) for the cart mass and spring stiffness should be done using the Least-Squares method, which finds values for m_i and k that minimize the squared error between the left and right sides of the equation.

Now that the spring constant has been obtained finding the other parameters is relatively straight forward. By comparing the second terms in (2.3) and (2.4) we find

$$\frac{c_i}{k} = \frac{2\zeta_i}{\omega_{ni}} \tag{2.21}$$

which may be rewritten in matrix-vector form as

$$\begin{bmatrix} 1 & 0 & 0 & 0 & -\frac{2\zeta_1}{\omega_{n1}} \\ 0 & 1 & 0 & 0 & -\frac{2\zeta_2}{\omega_{n2}} \\ 0 & 0 & 1 & 0 & -\frac{2\zeta_3}{\omega_{n3}} \\ 0 & 0 & 0 & 1 & -\frac{2\zeta_4}{\omega_{n4}} \\ 0 & 0 & 0 & 0 & 1 \end{bmatrix} \begin{Bmatrix} c_1 \\ c_2 \\ c_3 \\ c_4 \\ k \end{Bmatrix} = \begin{Bmatrix} 0 \\ 0 \\ 0 \\ 0 \\ k \end{Bmatrix} \tag{2.22}$$

This system is 5×5 upper triangular and should be solved by back substitution to determine the values of the damping constant.

Finally the hardware gain is computed in much the same manner as the damping constant. Comparing the coefficients in (2.3) and (2.4) we find

$$\frac{C_{hw}}{k} = K \tag{2.23}$$

Rearranging this into matrix vector form we find

$$\begin{bmatrix} 1 & 0 & 0 & 0 & -K_1 \\ 0 & 1 & 0 & 0 & -K_2 \\ 0 & 0 & 1 & 0 & -K_3 \\ 0 & 0 & 0 & 1 & -K_4 \\ 0 & 0 & 0 & 0 & 1 \end{bmatrix} \begin{Bmatrix} C_{hw_1} \\ C_{hw_2} \\ C_{hw_3} \\ C_{hw_4} \\ k \end{Bmatrix} = \begin{Bmatrix} 0 \\ 0 \\ 0 \\ 0 \\ k \end{Bmatrix} \tag{2.24}$$

Again this system is 5×5 upper triangular and should be solved by back substitution to determine the values of the hardware gain.

During the frequency response the cart's equation of motion is

$$m\ddot{x} = C_{hw} g(t) \tag{2.25}$$

making the transfer function

$$G(s) = \frac{C_{hw}}{ms^2} \tag{2.26}$$

We desire the Bode gain of the system which is found at the poles of the transfer function

$$K_{\text{Bode}} = \frac{C_{hw}}{m} \tag{2.27}$$

2.4 Sample Results

Although the particular system characteristics may vary from lab station to lab station the values found while developing this series of laboratories are shown in Tables 2.3 and 2.4.

Table 2.3: System Parameters for Cart 1

Case	m_{ti} (kg)	c_i (Ns/m)	k (N/m)	C_{hw_i}
1	2.2754	8.4623	741.1544	7212.4
2	1.7869	7.1077	741.1544	7394.5
3	1.3053	6.2053	741.1544	7458.6
4	0.7435	4.6603	741.1544	7475.7

Table 2.4: System Parameters for Cart 2

Case	m_{ti} (kg)	c_i (Ns/m)	k (N/m)	C_{hw_i}
1	2.0595	7.3801	326.6935	6203.7
2	1.5162	6.0157	326.6935	6301.8
3	1.0746	5.2893	326.6935	6389.6
4	0.5926	4.9804	326.6935	6355.3

Plots comparing the theoretical step response to the hardware implementation for the first cart can be seen in Figures 2.5-2.8.

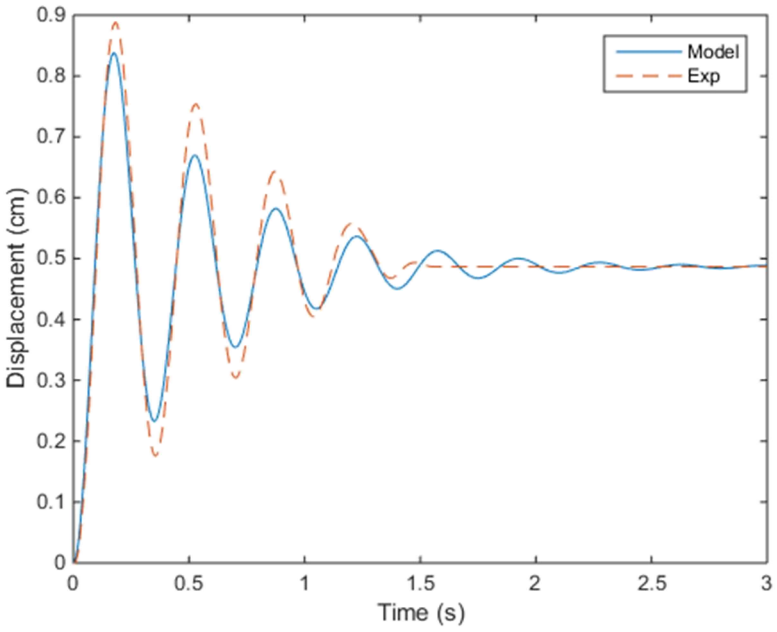

Figure 2.5: Comparison of the Theoretical and Expiremental Step response for case 1

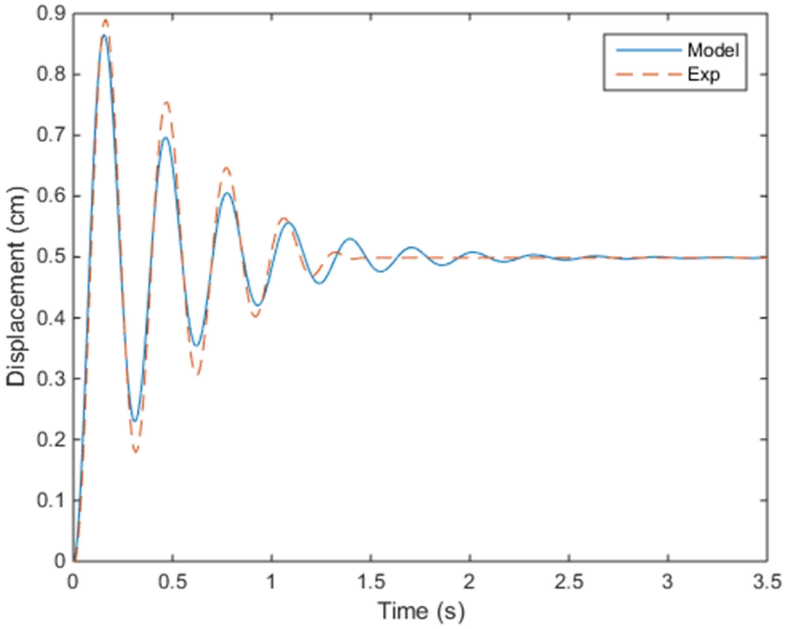

Figure 2.6: Comparison of the Theoretical and Expiremental Step response for case 2

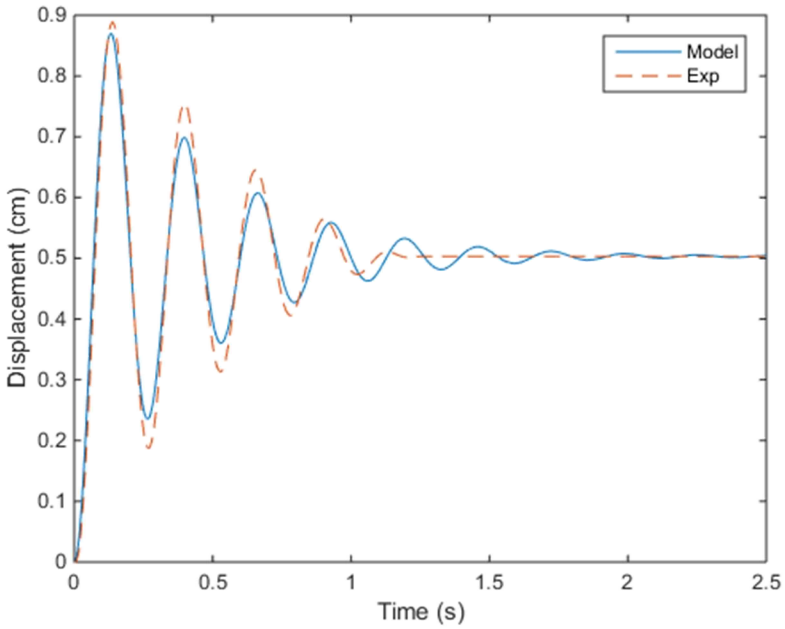

Figure 2.7: Comparison of the Theoretical and Expiremental Step response for case 3

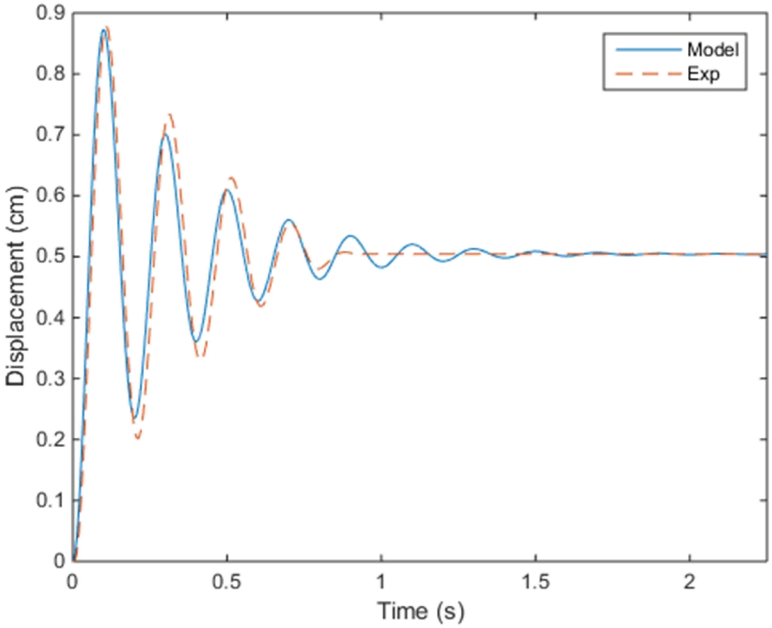

Figure 2.8: Comparison of the Theoretical and Expiremental Step response for case 4

Plots comparing the theoretical step response to the hardware implementation for the second cart can be seen in Figures 2.9-2.12.

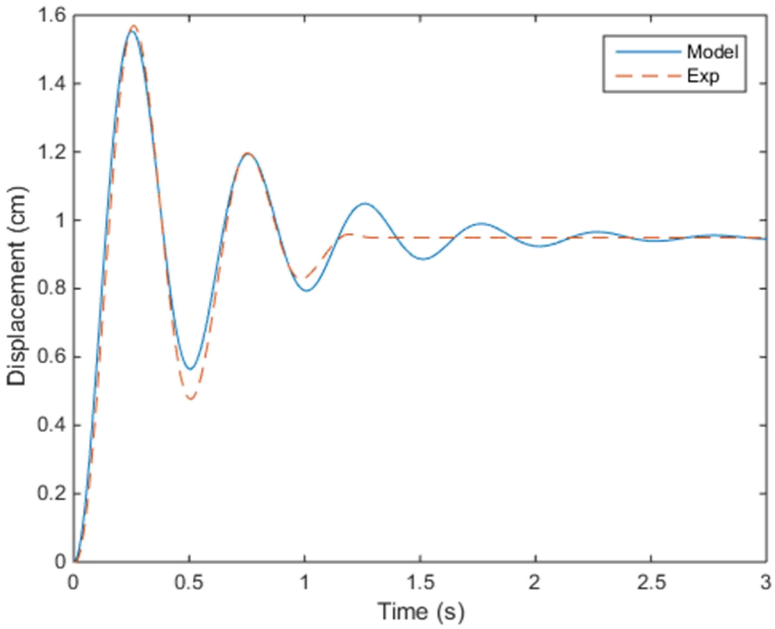

Figure 2.9: Comparison of the Theoretical and Expiremental Step response for case 1

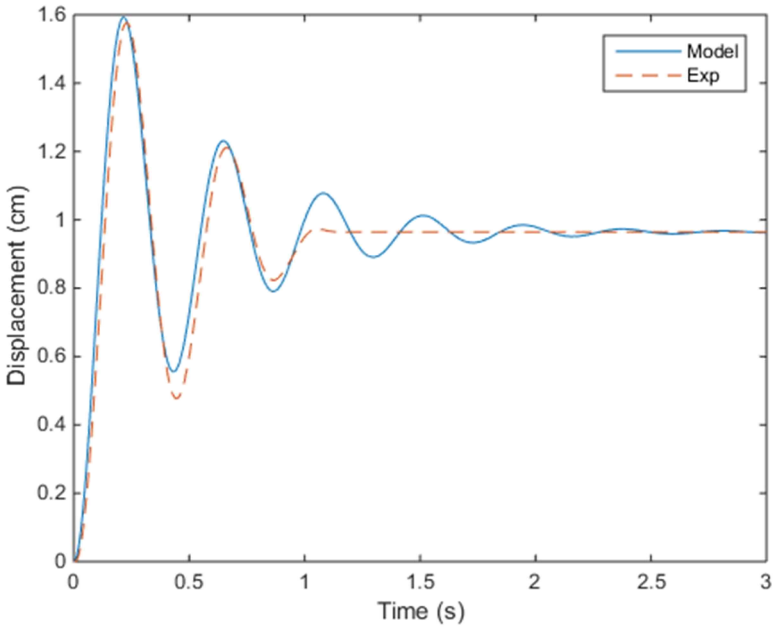

Figure 2.10: Comparison of the Theoretical and Expiremental Step response for case 2

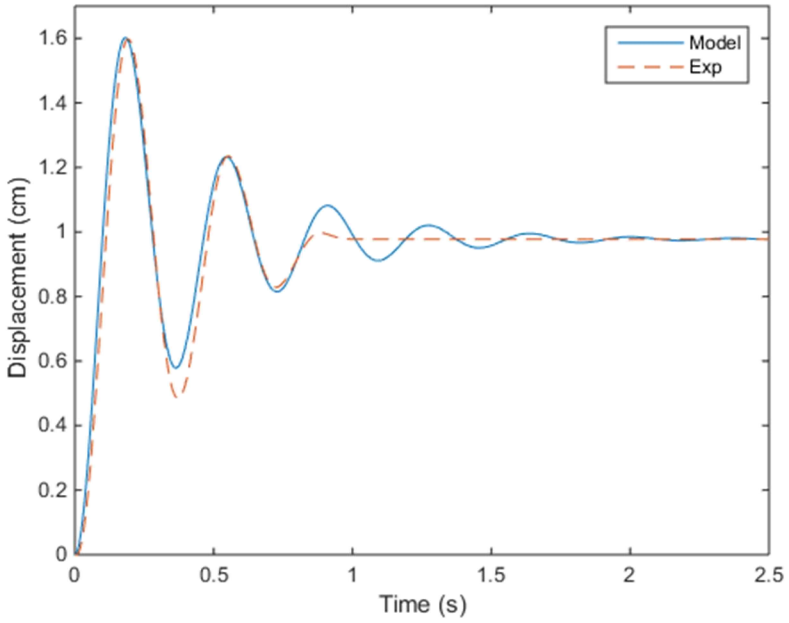

Figure 2.11: Comparison of the Theoretical and Expiremental Step response for case 3

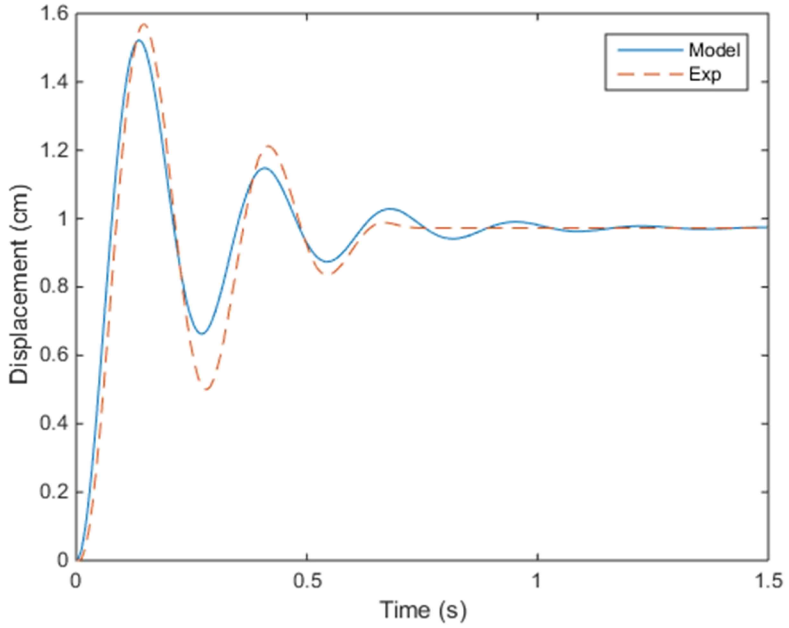

Figure 2.12: Comparison of the Theoretical and Expiremental Step response for case 4

The magnitudes found from the frequency response can be seen in Table 2.5

Table 2.5: Magnitudes

Case	Magnitude (dB)	Frequency (Hz)
1	25	3
2	19.28	4
3	15.2	5
4	12.05	6
5	9.03	7
6	6.6	8

The plot of the magnitudes can be seen in Figure 2.13

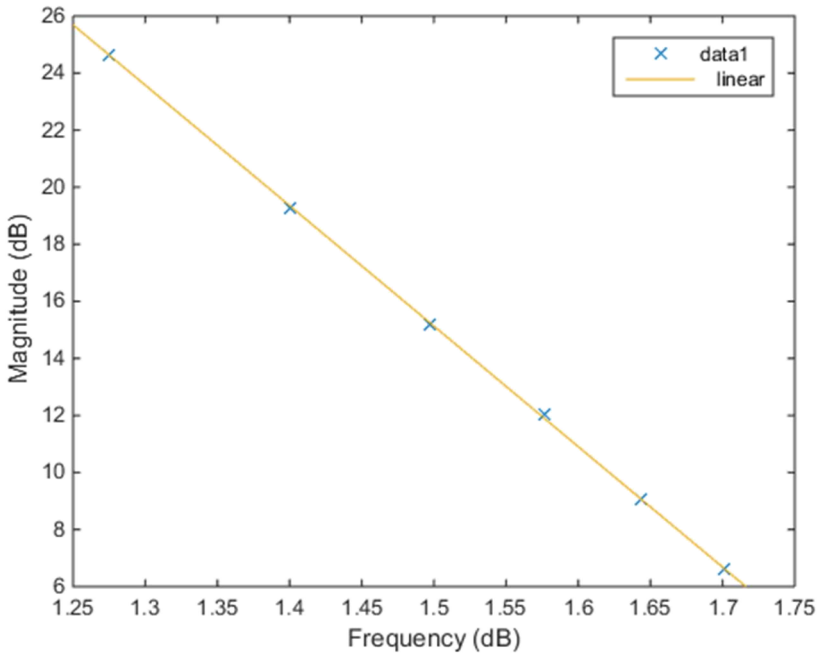

Figure 2.13: Response magnitude plotted against frequency

The line of best fit, given by MATLAB's plot fitter, is

$$y = -42.237x + 78.485 \tag{2.28}$$

where y, is the magnitude in dB and x is the input frequency in dB. This slope is close to our expected result. Since the transfer function is given by (2.26)

$$G(j\omega) = \frac{C_{hw}}{m\omega^2} \tag{2.29}$$

it can be shown that

$$|20\log_{10} G(j\omega)| = -40\left(\log_{10}\frac{C_{hw}}{m}\right)(\log_{10}\omega) \tag{2.30}$$

giving the expected result from a double integrator of a $-40\,\frac{\text{dB}}{\text{dec}}$. The intercept of this function is considered to be the Bode gain because Figure 2.13 is a linearized Bode plot and the poles of the transfer function are only at the origin. Also, Table 2.4 shows that for 1 added mass the total mass of the cart is approximately 1 $[kg]$ so it is assumed that the mass term in (2.29) is 1 $[kg]$. Converting the intercept from dB, the Bode gain is found to be

$$K_{\text{Bode}} = 8399.433 \tag{2.31}$$

3. DECOUPLING BY EIGENSTRUCTURE ASSIGNMENT

3.1 Experiment Goals

The main goal of this laboratory is to design and implement a controller to decouple a two degree of freedom system. In order to do so the system must be analyzed and state matrices formed. Then students should use the method of eigenstructure assignment put forward by Andry et al. to design a controller to decouple the two carts from each other [8].

3.2 Experimental Procedure

The experiment again involves using the ECP210, shown in Figure 1.1, this time configured in a two-degree-of-freedom set-up as represented below in Figure 3.1.

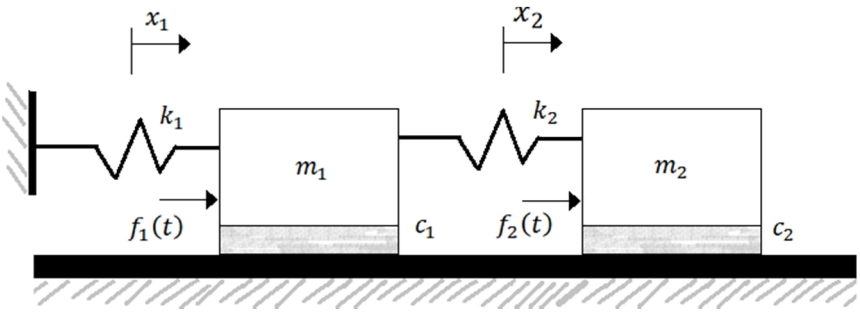

Figure 3.1: Model of the two degree of freedom system

In Figure 3.1, m_1 is the total mass of the first cart, m_2 is the total mass of the second cart, k_1 is the spring constant of the light spring, k_2 is the spring constant of the stiff spring, c_1 is the viscous damping constant of the first cart, c_2 is the viscous damping constant of the second cart, x_1 is the displacement of the first cart and x_2 is the displacement of the second cart. It should be

remembered that the inputs $f_1(t)$ and $f_2(t)$ are not what is specified in the Simulink block and should be rewritten by way of (2.2) that is

$$f_1(t) = C_{hw_1} g_1(t) \tag{3.1}$$
$$f_2(t) = C_{hw_2} g_2(t) \tag{3.2}$$

After the equations of motion have been found for the system, a choice of the system parameters should be made from the various cases from Chapter 1. Following this, the system should be represented in state-space form as a system of n states, p inputs and q outputs such that:

$$\dot{\mathbf{x}} = \mathbf{A}\mathbf{x} + \mathbf{B}\mathbf{u} \tag{3.3}$$
$$\mathbf{y} = \mathbf{C}\mathbf{x} \tag{3.4}$$

where $\mathbf{x}$ is the state vector and is $n \times 1$, $\mathbf{u}$ is the input vector and is $p \times 1$, $\mathbf{y}$ is the output vector and is $q \times 1$, $\mathbf{A}$ is the state matrix and has dimensions $n \times n$, $\mathbf{B}$ is the input matrix and has dimensions $n \times p$, $\mathbf{C}$ is the output matrix and has dimensions $q \times n$, and $\dot{\mathbf{x}}$ is the state vector's time derivative:

$$\dot{\mathbf{x}} = \frac{d}{dt}\mathbf{x} \tag{3.5}$$

After the system is set up, a controller should be designed that decouples the two carts, which is described in the next section. Following this, a pre-filter gain should be applied to the reference input to control the steady-state error to the applied step response [9]. Once these steps have been completed a theoretical step response should be implemented in Simulink similar to Figure 3.2.

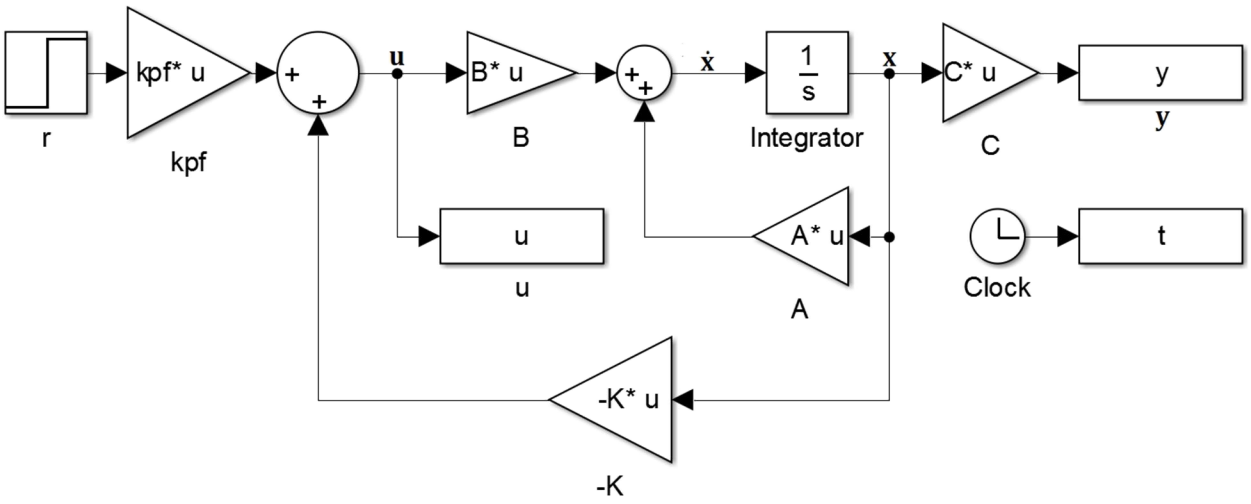

Figure 3.2: Simulink model of the two-degree-of-freedom system

In Figure 3.2, **r** is the reference input and $\mathbf{k_{pf}}$ is the pre-filter gain. After the theoretical model is constructed the system should be physically implemented on the ECP210.

3.3 Method of Analysis

The equations of motion of the two degree of freedom system shown in Figure 3.1 can be shown to be

$$m_1\ddot{x}_1 + c_1\dot{x}_1 + (k_1 + k_2)x_1 - k_2x_2 = f_1(t) \quad (3.6)$$
$$m_2\ddot{x}_2 + c_2\dot{x}_2 + k_2x_2 - k_2x_1 = f_2(t) \quad (3.7)$$

Substituting (3.1) and (3.2) into (3.6) and (3.7), respectively, the state-space system can be shown to be

$$\begin{Bmatrix} \dot{x}_1 \\ \ddot{x}_1 \\ \dot{x}_2 \\ \ddot{x}_2 \end{Bmatrix} = \begin{bmatrix} 0 & 1 & 0 & 0 \\ -\frac{(k_1+k_2)}{m_1} & -\frac{c_1}{m_1} & \frac{k_2}{m_1} & 0 \\ 0 & 0 & 0 & 1 \\ \frac{k_2}{m_2} & 0 & -\frac{k_2}{m_2} & -\frac{c_2}{m_2} \end{bmatrix} \begin{Bmatrix} x_1 \\ \dot{x}_1 \\ x_2 \\ \dot{x}_2 \end{Bmatrix} + \begin{bmatrix} 0 & 0 \\ \frac{C_{hw_1}}{m_1} & 0 \\ 0 & 0 \\ 0 & \frac{C_{hw_2}}{m_2} \end{bmatrix} \mathbf{u} \quad (3.8)$$

Using the control law

$$\mathbf{u} = -\mathbf{K}\mathbf{x} + \mathbf{k_{pf}}\mathbf{r} \tag{3.9}$$

where **K** is the controller gain, it is possible to rewrite (3.3) as

$$\dot{\mathbf{x}} = (\mathbf{A} - \mathbf{B}\mathbf{K})\mathbf{x} + \mathbf{B}\mathbf{k_{pf}}\mathbf{r} \tag{3.10}$$

From (3.10) we can obtain the closed-loop eigenvalue problem

$$(\mathbf{A} - \mathbf{B}\mathbf{K})\boldsymbol{\nu}_i = \lambda_i \boldsymbol{\nu}_i \tag{3.11}$$

where λ_i $(i = 1, 2, \dots, n)$ is a desired closed-loop eigenvalue and $\boldsymbol{\nu}_i$ is a closed-loop eigenvector. This can be rearranged to

$$[\lambda_i \mathbf{I} - \mathbf{A} \quad |\mathbf{B}] \begin{Bmatrix} \boldsymbol{\nu}_i \\ \boldsymbol{\theta}_i \end{Bmatrix} = \{\mathbf{0}\} \tag{3.12}$$

where

$$\boldsymbol{\theta}_i = \mathbf{K}\boldsymbol{\nu}_i \tag{3.13}$$

Let

$$\mu_i = \begin{Bmatrix} \boldsymbol{\nu}_i \\ \boldsymbol{\theta}_i \end{Bmatrix} \tag{3.14}$$

$$\mathbf{S}_i = [\lambda_i \mathbf{I} - \mathbf{A} \quad |\mathbf{B}] \tag{3.15}$$

To satisfy the eigenvalue problem, μ_i must lie in the nullspace of $\mathbf{S}_i$. The nullspace is given from the singular value decomposition where

$$\text{null}(\mathbf{S}_i) = \text{span}([\mathbf{v}_{r+1}, \dots, \mathbf{v}_z]) \tag{3.16}$$

where $\mathbf{v}$ is the right singular vector found by singular value decomposition, the subscript r represents the rank of the matrix $\mathbf{S}_i$, and the subscript z represents the number of right singular vectors. It is then desired to contrive μ_i for each λ_i as a linear combination of $\mathbf{v}_{r+1}, \ldots, \mathbf{v}_z$ such that the decoupling requirements are satisfied:

$$\mu_i = \alpha_{i1}\mathbf{v}_{r+1} + \cdots + \alpha_{iz-r}\mathbf{v}_z \tag{3.17}$$

where α_{ij} $(j = 1, 2, \ldots, z-r)$ is some scalar. Assuming that λ_i are distinct, $[\boldsymbol{\nu}_1 \quad \cdots \quad \boldsymbol{\nu}_n]$ is invertible and

$$\mathbf{K} = [\boldsymbol{\theta}_1 \quad \cdots \quad \boldsymbol{\theta}_n][\boldsymbol{\nu}_1 \quad \cdots \quad \boldsymbol{\nu}_n]^{-1} \tag{3.18}$$

Now that the closed loop gain of the system has been calculated, it is now desirable to calculate a pre-filter to help control the steady state error. Consider the control law

$$\mathbf{u} = -\mathbf{K}\mathbf{x} + \mathbf{r} \tag{3.19}$$

Which provides a reference input to the system, but the steady state error of the system will be non-zero. If the desired values of the state and the control are $\mathbf{x}_{ss}$ and $\mathbf{u}_{ss}$ then the control should be

$$\mathbf{u} = -\mathbf{K}\mathbf{x} + \mathbf{k}_{\mathbf{pf}}\mathbf{r} \tag{3.20}$$

Where $\mathbf{k}_{\mathbf{pf}}$ is determined such that the system will have zero steady-state error to any constant input. In the steady state (3.3) and (3.4) reduce to

$$\mathbf{0} = \mathbf{A}\mathbf{x}_{ss} + \mathbf{B}\mathbf{u}_{ss} \tag{3.21}$$

$$\mathbf{y}_{ss} = \mathbf{C}\mathbf{x}_{ss} \tag{3.22}$$

It is desirable to solve for the values where

$$\mathbf{y}_{ss} = \mathbf{r}_{ss}, \forall \mathbf{r}_{ss} \tag{3.23}$$

To do this we set

$$\mathbf{x}_{ss} = \mathbf{N}_x \mathbf{r}_{ss} \tag{3.24}$$

$$\mathbf{u}_{ss} = \mathbf{N}_u \mathbf{r}_{ss} \tag{3.25}$$

substituting (3.24) and (3.25) into (3.21) and (3.22) and rewriting as a matrix equation yields:

$$\begin{bmatrix} \mathbf{A} & \mathbf{B} \\ \mathbf{C} & \mathbf{0} \end{bmatrix} \begin{bmatrix} \mathbf{N}_x \\ \mathbf{N}_u \end{bmatrix} = \begin{bmatrix} \mathbf{0} \\ \mathbf{I} \end{bmatrix} \tag{3.26}$$

where $\mathbf{I}$ is an identity matrix of size p. After solving for $\mathbf{N}_x$ and $\mathbf{N}_u$ the control law can be written as

$$\mathbf{u} = -\mathbf{K}(\mathbf{x} - \mathbf{N}_x \mathbf{r}) + \mathbf{N}_u \mathbf{r} \tag{3.27}$$

Rearraging (3.27) and comparing to (3.20), $\mathbf{k_{pf}}$ can be shown to be [8]

$$\mathbf{k_{pf}} = (\mathbf{N}_u + \mathbf{K}\mathbf{N}_x) \tag{3.28}$$

3.4 Sample Calculation and Results

The system characteristics used to develop this laboratory are shown in Table 3.1.

Table 3.1: Parameters Used

Cart	m_{ti} (kg)	c_i (Ns/m)	k_i (N/m)	C_{hw_i}
1	2.275	8.5	326.7	7212.4
2	2.06	7.4	741.2	6203.7

This leads the system matrices to be

$$\mathbf{A} = \begin{bmatrix} 0 & 1 & 0 & 0 \\ -469.3 & -3.72 & 325.7 & 0 \\ 0 & 0 & 0 & 1 \\ 359.9 & 0 & -359.9 & -3.58 \end{bmatrix} \tag{3.29}$$

$$\mathbf{B} = \begin{bmatrix} 0 & 0 \\ 3167 & 0 \\ 0 & 0 \\ 0 & 3012 \end{bmatrix} \tag{3.30}$$

$$\mathbf{C} = \begin{bmatrix} 1 & 0 & 0 & 0 \\ 0 & 0 & 1 & 0 \end{bmatrix} \tag{3.31}$$

Only two eigenvalues need to be assigned to decouple the system; the other two eigenvalues will come out as the complex conjugates of the assigned eigenvalues. Assigned poles should be kept away from natural eigenvalues as well as away from the origin in the left-hand plane, i.e., they should have fast responses. For this example the values in Table 3.2 were selected.

Table 3.2: Assigned Eigenvalues

Cart	λ_i
1	$-4 \pm j11$
2	$-3 \pm j21$

After forming the singular value decomposition the values of μ_i need to be contrived in order to decouple the system:

$$\mu_1 = \begin{Bmatrix} \times \\ \times \\ 0 \\ 0 \\ \hline \boldsymbol{\theta}_1 \end{Bmatrix} = \alpha_{11}\mathbf{v}_{1_5} + \alpha_{12}\mathbf{v}_{1_6} \tag{3.32}$$

$$\mu_2 = \begin{Bmatrix} 0 \\ 0 \\ \times \\ \times \\ \hline \boldsymbol{\theta}_2 \end{Bmatrix} = \alpha_{21}\mathbf{v}_{2_5} + \alpha_{22}\mathbf{v}_{2_6} \tag{3.33}$$

where $\times$ is some number that will come about as a result of contriving values of μ_i. Now (3.32) and (3.33) should be rewritten as

$$\begin{bmatrix} \mathrm{v}1_{3,5} & \mathrm{v}1_{3,6} \\ \mathrm{v}1_{4,5} & \mathrm{v}1_{4,6} \end{bmatrix} \begin{Bmatrix} \alpha_{11} \\ \alpha_{12} \end{Bmatrix} = \begin{Bmatrix} 0 \\ 0 \end{Bmatrix} \tag{3.34}$$

$$\begin{bmatrix} \mathrm{v}2_{1,5} & \mathrm{v}2_{1,6} \\ \mathrm{v}2_{2,5} & \mathrm{v}2_{2,6} \end{bmatrix} \begin{Bmatrix} \alpha_{21} \\ \alpha_{22} \end{Bmatrix} = \begin{Bmatrix} 0 \\ 0 \end{Bmatrix} \tag{3.35}$$

from (3.34) and (3.35) it is obvious that the values of α are the null space of the appropriate matrix. For the this example μ_1 and μ_2 were found to be

$$\mu_1 = \begin{Bmatrix} -.0309 - j0.0793 \\ 0.996 - j0.0227 \\ 0 \\ 0 \\ \hline 0.0046 + j0.0083 \\ -0.0037 - j0.0095 \end{Bmatrix} \tag{3.36}$$

$$\mu_2 = \begin{Bmatrix} 0 \\ 0 \\ 0.047 - j0.003 \\ -0.2034 - j0.978 \\ \hline 0.0048 - j0.0003 \\ 0.0012 - j0.0009 \end{Bmatrix} \tag{3.37}$$

After solving (3.18) **K** is found to be

$$\mathbf{K} = \begin{bmatrix} -0.1048 & 0.0014 & 0.1028 & 0 \\ 0.1195 & 0 & 0.0299 & 0.0008 \end{bmatrix} \tag{3.38}$$

Now that **K** has been found, solving (3.26), $\mathbf{N}_u$ and $\mathbf{N}_x$ are found to be

$$\mathbf{N}_u = \begin{bmatrix} 0.1481 & -0.1028 \\ -0.1195 & 0.1195 \end{bmatrix} \tag{3.39}$$

$$\mathbf{N}_x = \begin{bmatrix} 1 & 0 \\ 0 & 0 \\ 0 & 1 \\ 0 & 0 \end{bmatrix} \tag{3.40}$$

Solving (3.28),

$$\mathbf{k_{pf}} = \begin{bmatrix} 0.0432 & 0 \\ 0 & 0.1494 \end{bmatrix} \tag{3.41}$$

A plot of the theoretical decoupling can be seen in Figure 3.3.

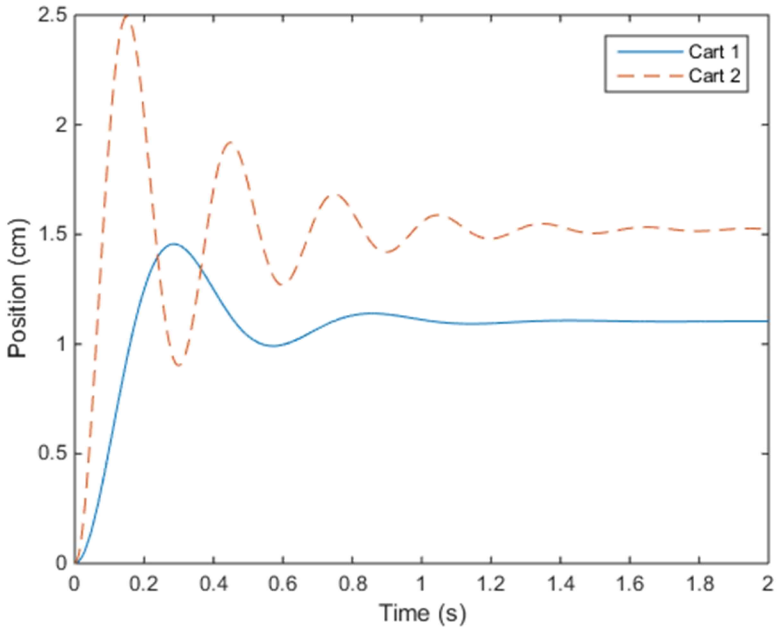

Figure 3.3: Theoretical response of the system

The actual response can be seen in Figure 3.4.

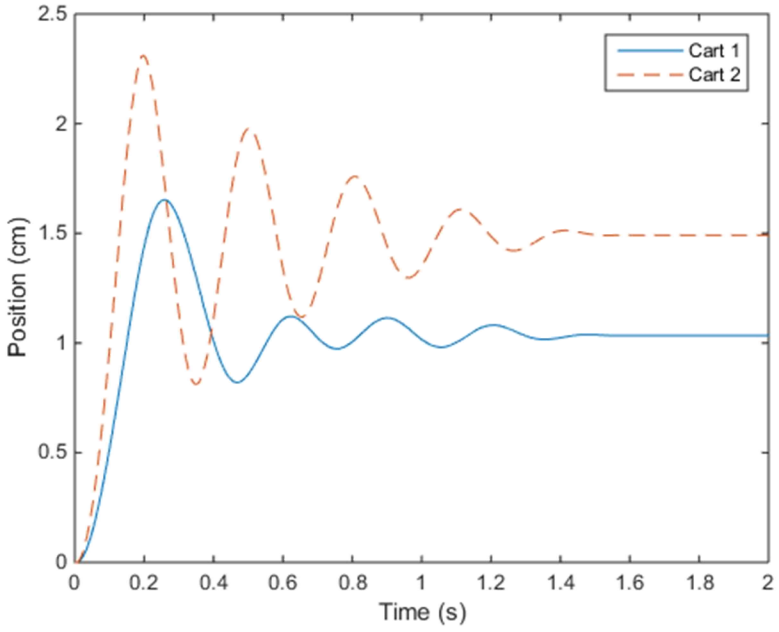

Figure 3.4: Actual response of the system

A comparison between the theoretical and actual cart responses can be seen in Figures 3.5-3.6.

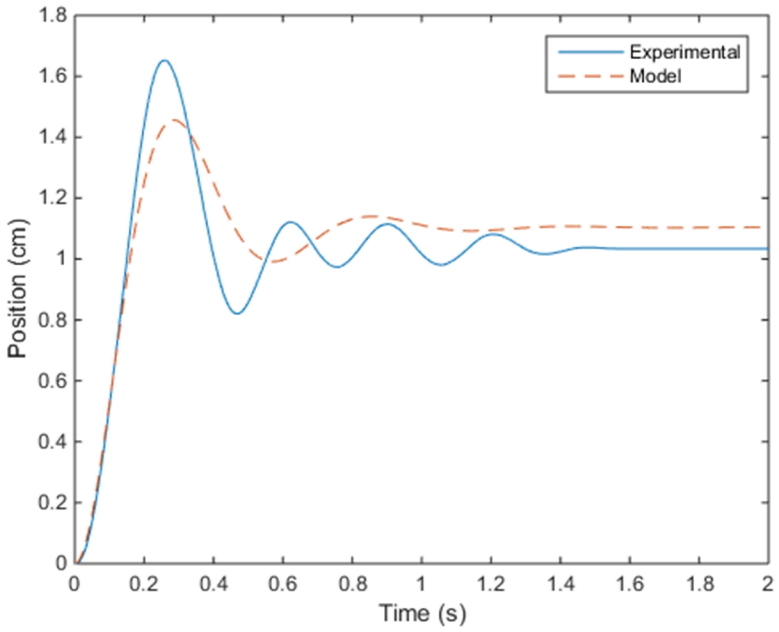

Figure 3.5: Comparison of Cart 1's theoretical and actual responses

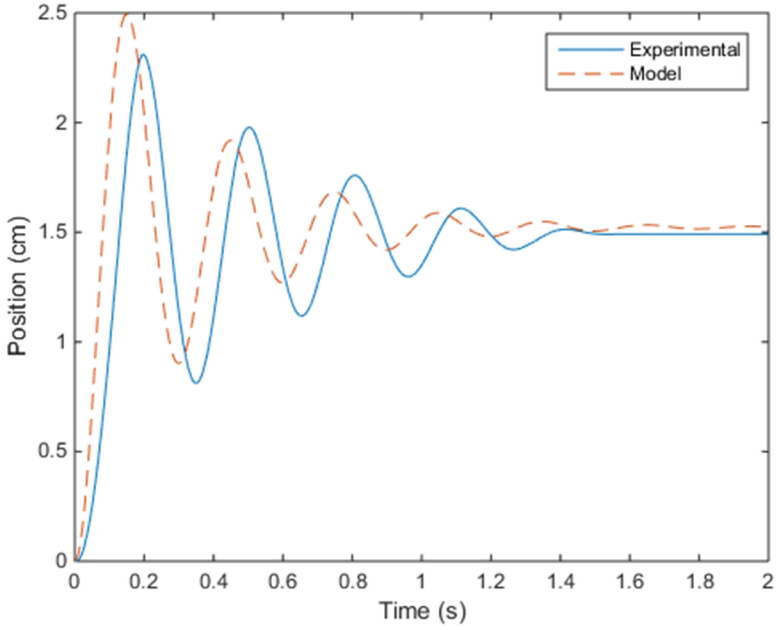

Figure 3.6: Comparison of Cart 2's theoretical and actual responses

The system is not perfectly decoupled; as seen in Figure 3.5, the second cart is influencing the first. This is due to imperfections in the model.

4. LINEAR OPTIMAL REGULATOR

4.1 Experiment Goals

The main goal of this laboratory is to implement a finite horizon linear optimal regulator (LOR). This regulator will solve a simple single-input single-output optimal control problem. This laboratory will also serve to highlight the flaws in the assumption that our system is only acted on by viscous friction.

4.2 Experimental Procedure

This experiment once again utilizes the ECP210 system. This time, however the system is set up utilizing just the second cart, a single 500 g mass and the hardware gain found from the frequency response in Chapter 2. The representative system is shown in Figure 4.1

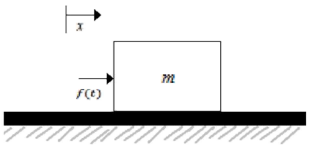

Figure 4.1: Single Mass Cart System

where m is approximately unity [kg] and $f(t)$ is given by

$$f(t) = Ku(t) \tag{4.1}$$

where K is the Bode gain found from Chapter 2. Like the frequency response, this system is treated as having negligible viscous damping. The state equation for this system is

$$\dot{\mathbf{x}} = \mathbf{A}\mathbf{x} + \mathbf{B}u(t) \tag{4.2}$$

In matrix-vector form (4.1) can be written as

$$\begin{Bmatrix} \dot{x} \\ \ddot{x} \end{Bmatrix} = \begin{bmatrix} 0 & 1 \\ 0 & 0 \end{bmatrix} \begin{Bmatrix} x \\ \dot{x} \end{Bmatrix} + \begin{bmatrix} 0 \\ K \end{bmatrix} u(t) \tag{4.3}$$

The optimal control effort $u(t)$ to return the mass to zero position from an arbitrary starting point can be calculated as

$$u(t) = -\mathrm{R}^{-1}\mathbf{B}^T\boldsymbol{\lambda}(t) \tag{4.4}$$

where R is the penalty on the control effort and a scalar, and $\boldsymbol{\lambda}(t)$ is the costate. With this information, as well as information in the next section, a simulation can be created such as the one shown in Figure 4.2.

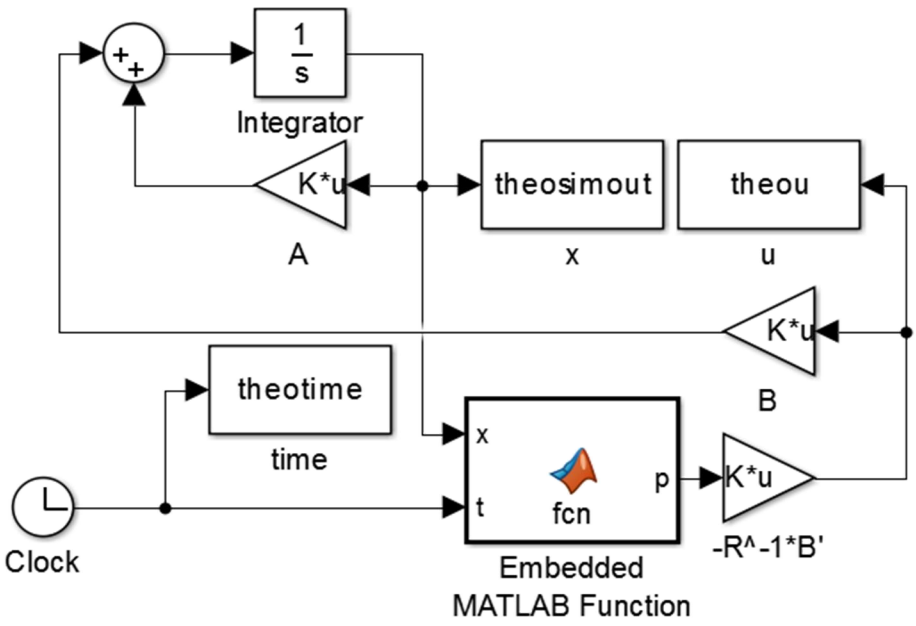

Figure 4.2: LOR Simulink Block Diagram

An embedded MATLAB function is necessary to calculate the costate in real time. R should initially be set as

$$\mathrm{R} = \|\mathbf{B}\|_2^2 \tag{4.5}$$

This will produce little to no effort from the controller, but serves as a base point from which to find a value for R that minimizes steady-state error without amplifying sensor noise.

4.3 Method of Analysis

The chosen cost function is

$$J = \frac{1}{2}\mathbf{x}^T(t_f)\mathbf{S}\mathbf{x}(t_f) + \int_{t_o}^{t_f} \frac{1}{2}(\mathbf{x}^T\mathbf{Q}\mathbf{x} + u^T\mathrm{R}u)\, dt \tag{4.6}$$

where $\mathbf{Q}$ is the penalty on the transient state deviation, $\mathbf{S}$ is the penalty on the finite state, t_f is the final time, t_o is the initial time and J is the performance index. It should be noted that $\mathbf{S}$ and $\mathbf{Q}$ are positive semi-definite $n \times n$ matrices.

The corresponding Hamiltonian function is

$$H = \frac{1}{2}(\mathbf{x}^T\mathbf{Q}\mathbf{x} + u^T\mathrm{R}u) + \boldsymbol{\lambda}^T(\mathbf{A}\mathbf{x} + \mathbf{B}u) \tag{4.7}$$

The Euler-Lagrange equations are

$$\dot{\boldsymbol{\lambda}} = -\frac{\partial H}{\partial t} = -\mathbf{Q}\mathbf{x} - \mathbf{A}^T\boldsymbol{\lambda} \tag{4.8}$$

$$\frac{\partial H}{\partial u} = \mathbf{0} \rightarrow \mathbf{0} = \mathrm{R}u + \mathbf{B}^T\boldsymbol{\lambda} \tag{4.9}$$

and

$$\boldsymbol{\lambda}(t_f) = \mathbf{S}\mathbf{x}(t_f) \tag{4.10}$$

Choosing R $>$ 0 the control law is given by (4.4). By substituting (4.4) into the state equation (4.2) and concatenating the state and costate equation (4.8), a $2n \times 2n$ system can be obtained:

$$\begin{Bmatrix} \dot{\mathbf{x}} \\ \dot{\boldsymbol{\lambda}} \end{Bmatrix} = \begin{bmatrix} \mathbf{A} & -\mathbf{B}\mathrm{R}^{-1}\mathbf{B}^T \\ -\mathbf{Q} & -\mathbf{A}^T \end{bmatrix} \begin{Bmatrix} \mathbf{x} \\ \boldsymbol{\lambda} \end{Bmatrix} \tag{4.11}$$

By substituting (4.10) into (4.11), (4.11) may be solved using state transition matrices $\boldsymbol{\Theta}_{ij}$

$$\begin{Bmatrix} \mathbf{x}(t) \\ \boldsymbol{\lambda}(t) \end{Bmatrix} = \begin{bmatrix} \boldsymbol{\Theta}_{11} & \boldsymbol{\Theta}_{12} \\ \boldsymbol{\Theta}_{21} & \boldsymbol{\Theta}_{22} \end{bmatrix} \begin{Bmatrix} \mathbf{x}(t_f) \\ \mathbf{S}\mathbf{x}(t_f) \end{Bmatrix} \tag{4.12}$$

such that

$$\mathbf{x}(t_f) = (\boldsymbol{\Theta}_{11} + \boldsymbol{\Theta}_{12}\mathbf{S})^{-1}\mathbf{x}(t) \tag{4.13}$$

and

$$\boldsymbol{\lambda}(\boldsymbol{t}) = (\boldsymbol{\Theta}_{\boldsymbol{21}} + \boldsymbol{\Theta}_{\boldsymbol{22}}\mathbf{S})\mathbf{x}(\boldsymbol{t_f}) \tag{4.14}$$

Therefore the costate at any time t is

$$\boldsymbol{\lambda}(t) = (\boldsymbol{\Theta}_{21} + \boldsymbol{\Theta}_{22}\mathbf{S})(\boldsymbol{\Theta}_{11} + \boldsymbol{\Theta}_{12}\mathbf{S})^{-1}\mathbf{x}(t) \tag{4.15}$$

The state transition matrices can be found using the matrix exponential

$$\begin{bmatrix} \boldsymbol{\Theta}_{11} & \boldsymbol{\Theta}_{12} \\ \boldsymbol{\Theta}_{21} & \boldsymbol{\Theta}_{22} \end{bmatrix} = \exp \begin{bmatrix} \mathbf{A}\mathrm{T} & -\mathbf{B}\mathrm{R}^{-1}\mathbf{B}\mathrm{T} \\ \mathbf{Q}\mathrm{T} & -\mathbf{A}^T\mathrm{T} \end{bmatrix} \tag{4.16}$$

where

$$\mathrm{T} = t - t_f \tag{4.17}$$

It should be noted that (4.16) may not be taken in a piecewise fashion [10]. The closed form solution to (4.16) is

$$\begin{bmatrix} \boldsymbol{\Theta}_{11} & \boldsymbol{\Theta}_{12} \\ \boldsymbol{\Theta}_{21} & \boldsymbol{\Theta}_{22} \end{bmatrix} = \begin{bmatrix} 1 & -\frac{1}{2}e^{-\mathrm{T}} + \frac{1}{2}e^{\mathrm{T}} & -\frac{1}{2}e^{-\mathrm{T}} + \frac{1}{2}e^{\mathrm{T}} - \mathrm{T} & -\frac{1}{2}e^{-\mathrm{T}} - \frac{1}{2}e^{\mathrm{T}} + 1 \\ 0 & \frac{1}{2}e^{-\mathrm{T}} + \frac{1}{2}e^{\mathrm{T}} & \frac{1}{2}e^{-\mathrm{T}} + \frac{1}{2}e^{\mathrm{T}} - 1 & \frac{1}{2}e^{-\mathrm{T}} - \frac{1}{2}e^{\mathrm{T}} \\ 0 & 0 & 1 & 0 \\ 0 & \frac{1}{2}e^{-\mathrm{T}} - \frac{1}{2}e^{\mathrm{T}} & \frac{1}{2}e^{-\mathrm{T}} - \frac{1}{2}e^{\mathrm{T}} & \frac{1}{2}e^{-\mathrm{T}} + \frac{1}{2}e^{\mathrm{T}} \end{bmatrix} \tag{4.19}$$

This solution, (4.19), is implemented in the embedded MATLAB function block in both the theoretical simulation shown in Figure 4.2 and the actual Simulink RTW block diagram in Figure 4.3 below.

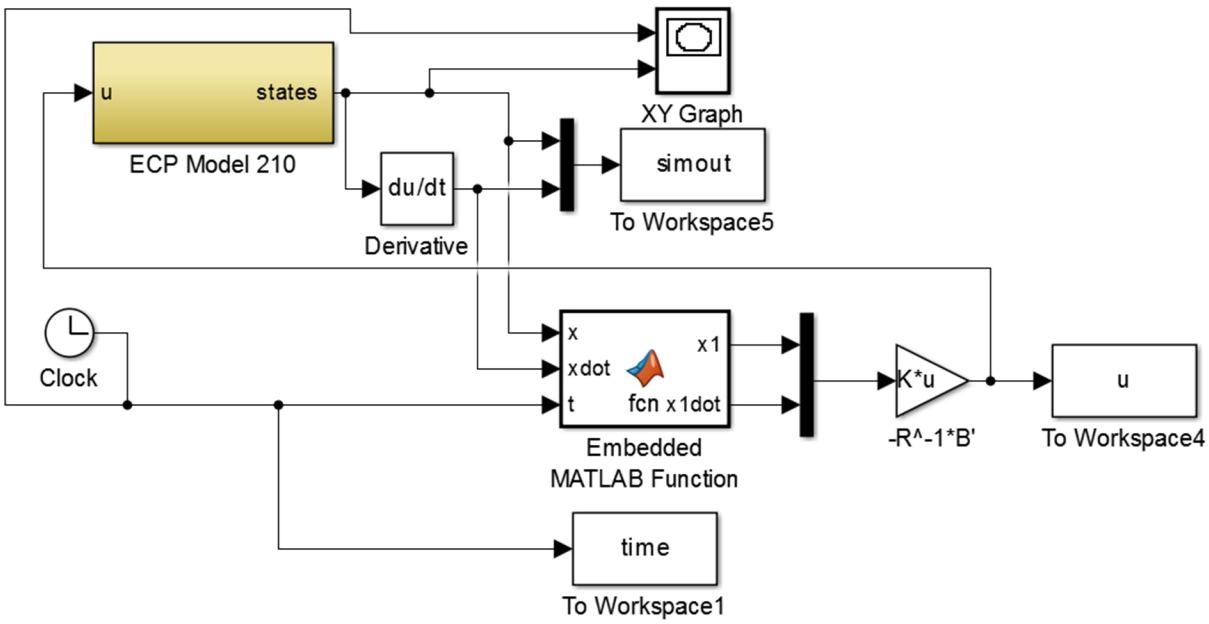

Figure 4.3: Simulink RTW Block Diagram

4.4 Sample Results

The final values of R and K used to develop this laboratory are shown in Table 4.1.

Table 4.1: Parameters Used

Case	K	R
1	10238	1.0489×10^8
2	10238	5.2405×10^6
3	10238	3.4936×10^6
4	10238	2.6202×10^6
5	10238	2.3291×10^6
6	10238	2.23×10^6
7	10238	2.139×10^6
8	10238	2.0962×10^6
9	10238	1.7468×10^6

Additionally, the **S** and **Q** matrices are

$$\mathbf{S} = \begin{bmatrix} 75 & 0 \\ 0 & 1 \end{bmatrix} \tag{4.18}$$

and

$$\mathbf{Q} = \begin{bmatrix} 0 & 0 \\ 0 & 1 \end{bmatrix} \tag{4.19}$$

Plots comparing the displacement and velocity of the theoretical response for the different cases of the hardware implementation can be seen in Figures 4.4-4.21.

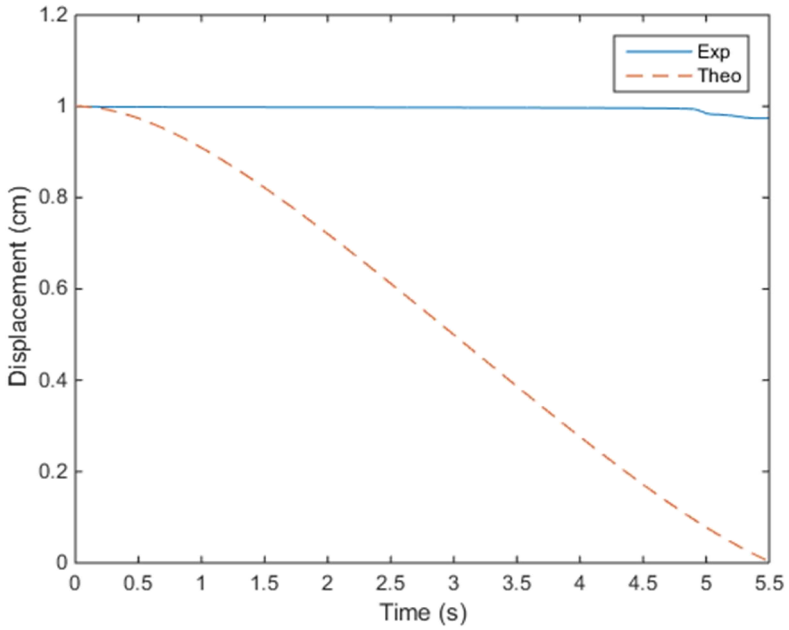

Figure 4.4: Case 1 Displacement Comparison

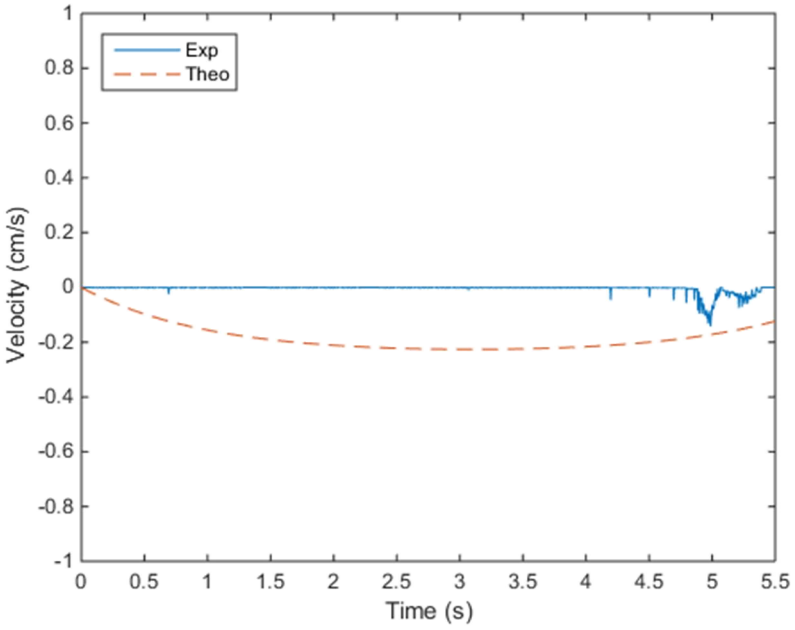

Figure 4.5: Case 1 Velocity Comparison

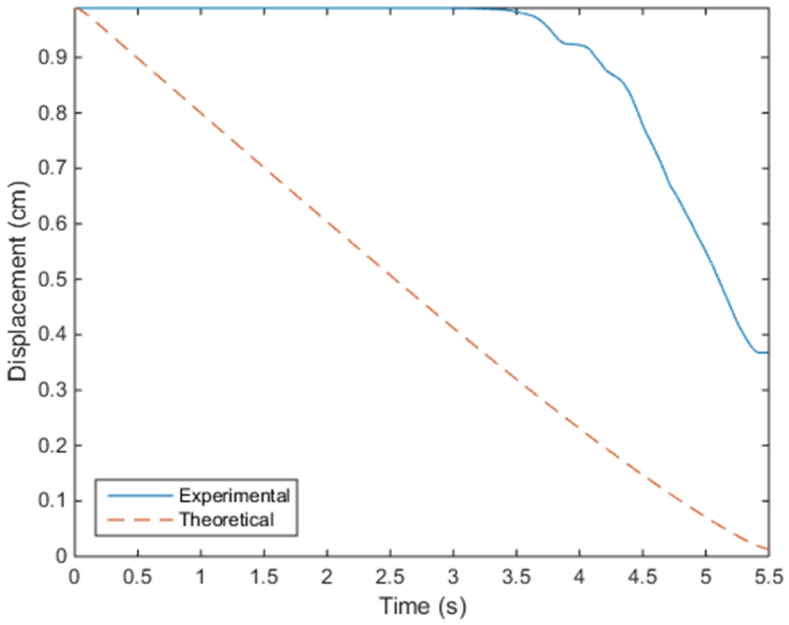

Figure 4.6: Case 2 Displacement Comparison

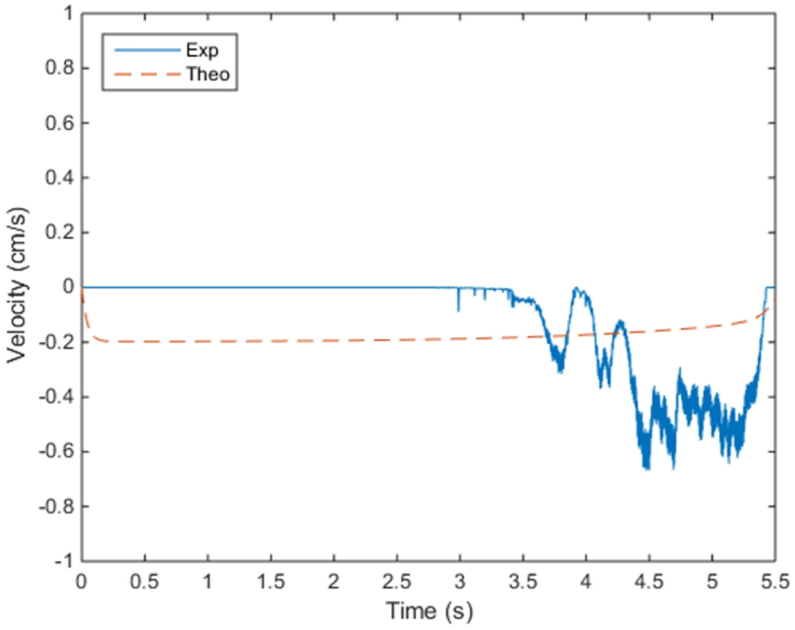

Figure 4.7: Case 2 Velocity Comparison

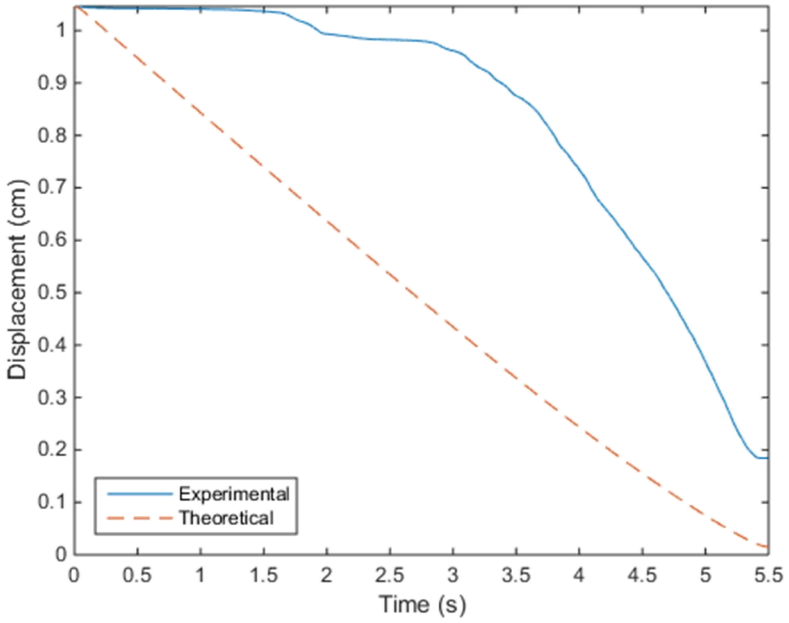

Figure 4.8: Case 3 Displacement Comparison

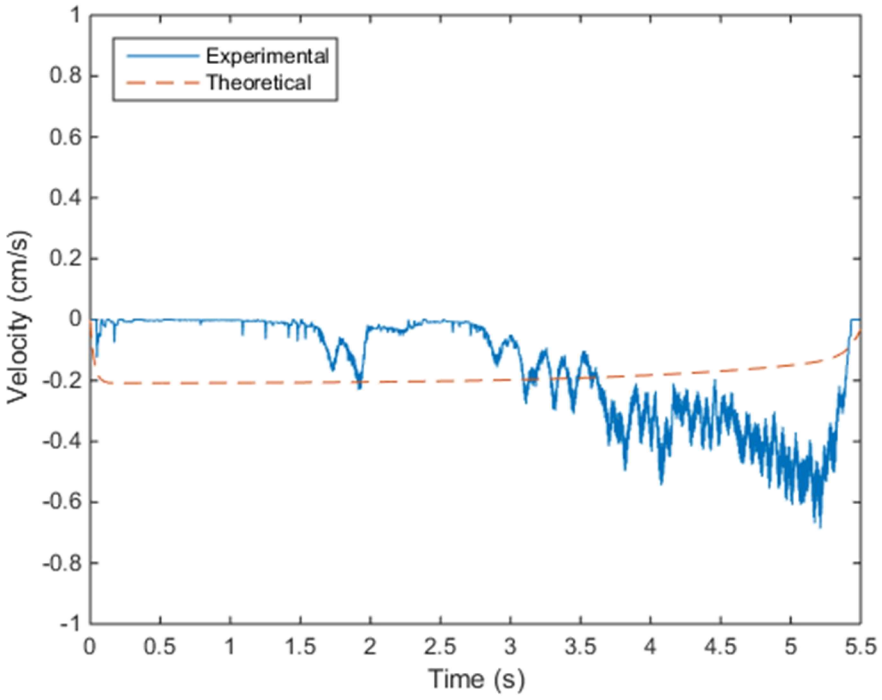

Figure 4.9: Case 3 Velocity Comparison

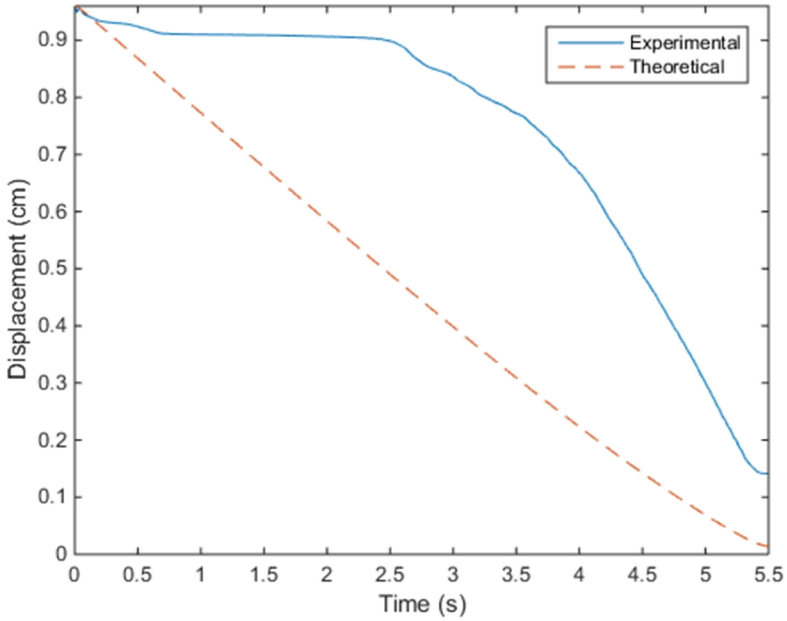

Figure 4.10: Case 4 Displacement Comparison

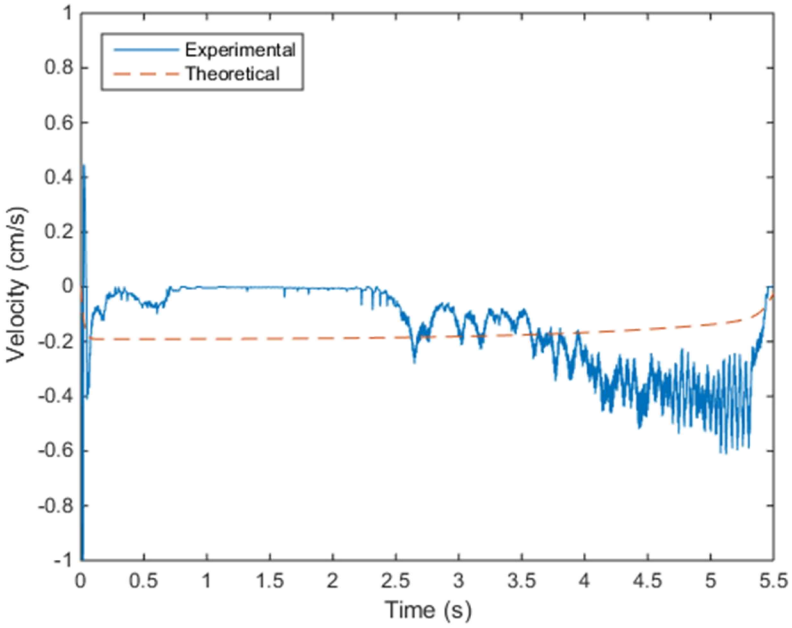

Figure 4.11: Case 4 Velocity Comparison

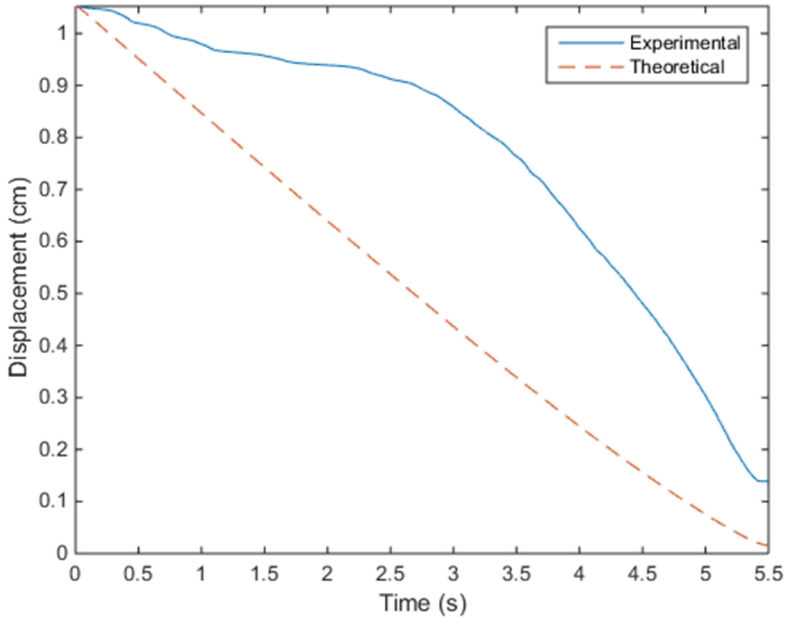

Figure 4.12: Case 5 Displacement Comparison

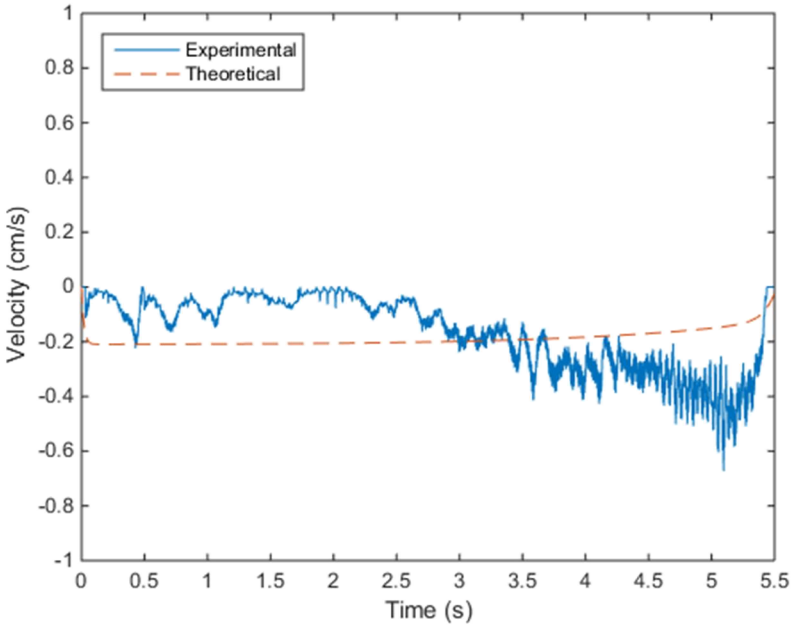

Figure 4.13: Case 5 Velocity Comparison

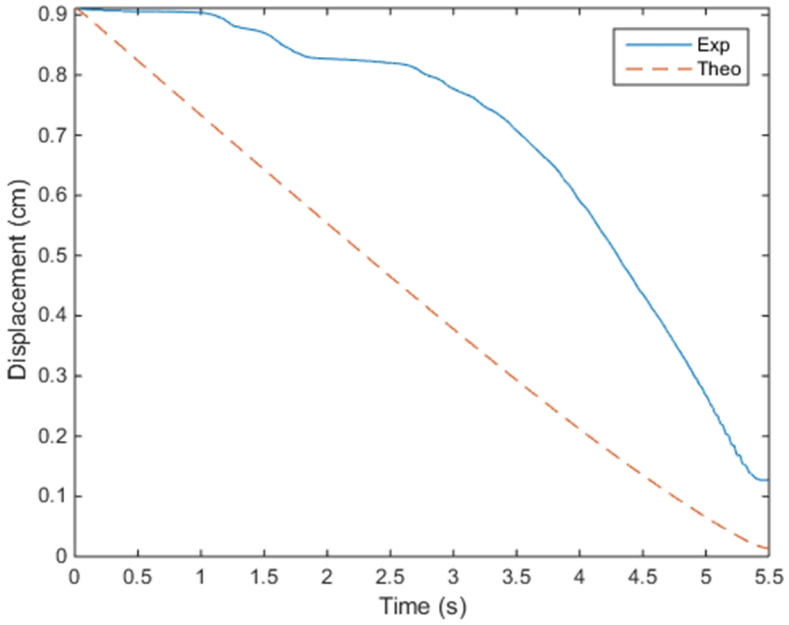

Figure 4.14: Case 6 Displacement Comparison

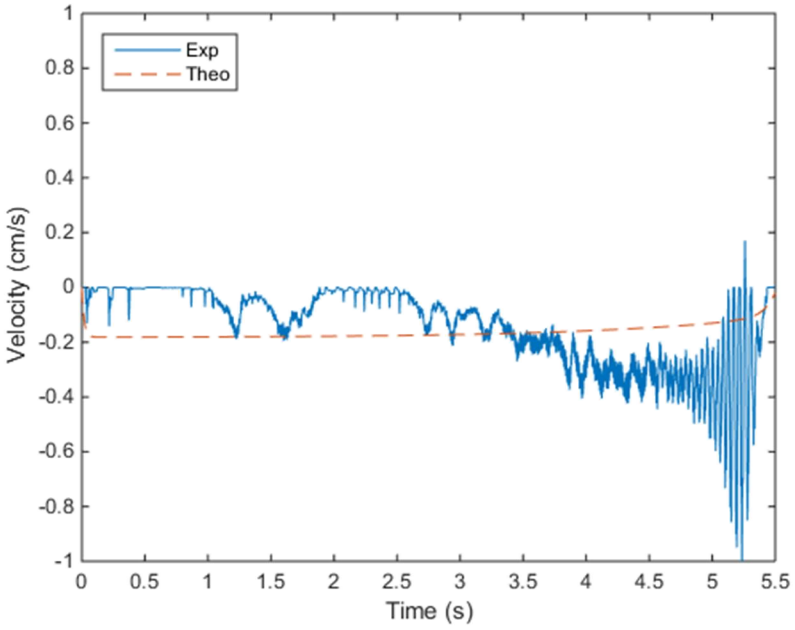

Figure 4.15: Case 6 Velocity Comparison

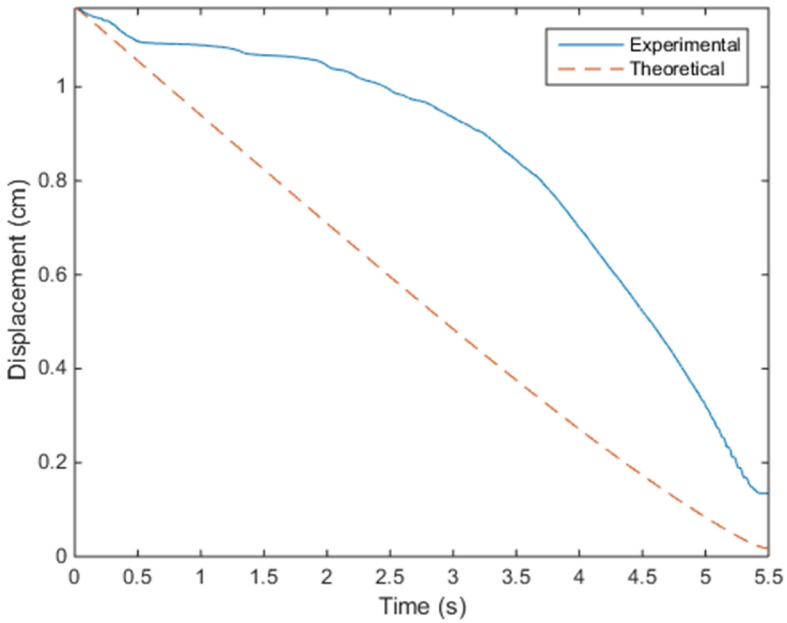

Figure 4.16: Case 7 Displacement Comparison

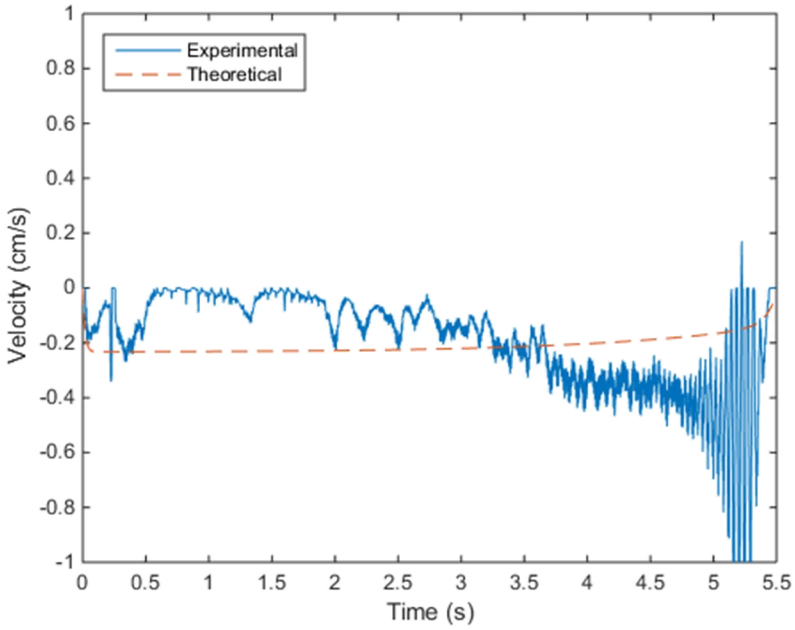

Figure 4.17: Case 7 Velocity Comparison

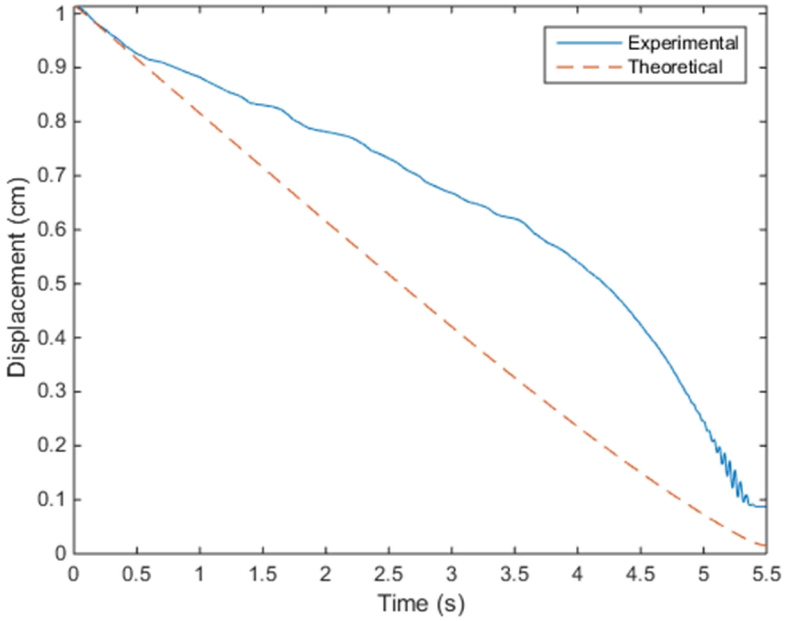

Figure 4.18: Case 8 Displacement Comparison

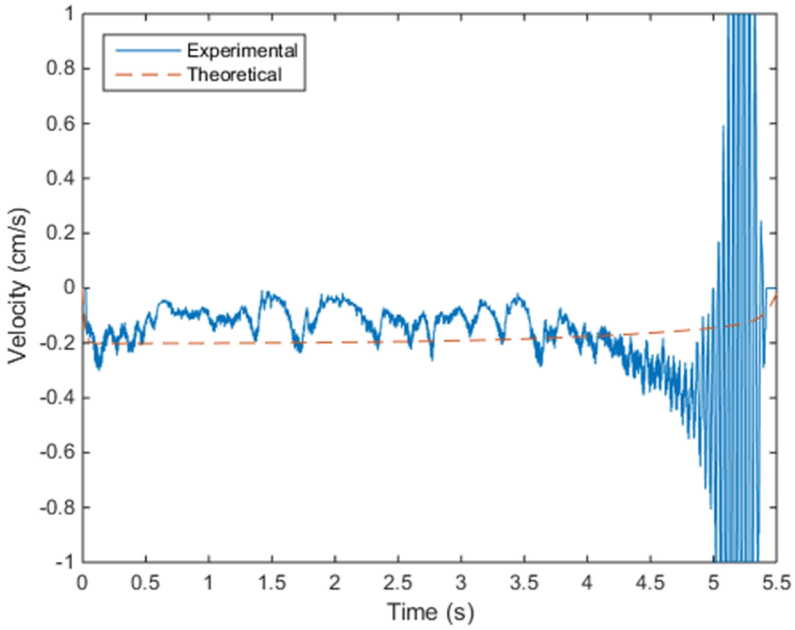

Figure 4.19: Case 8 Velocity Comparison

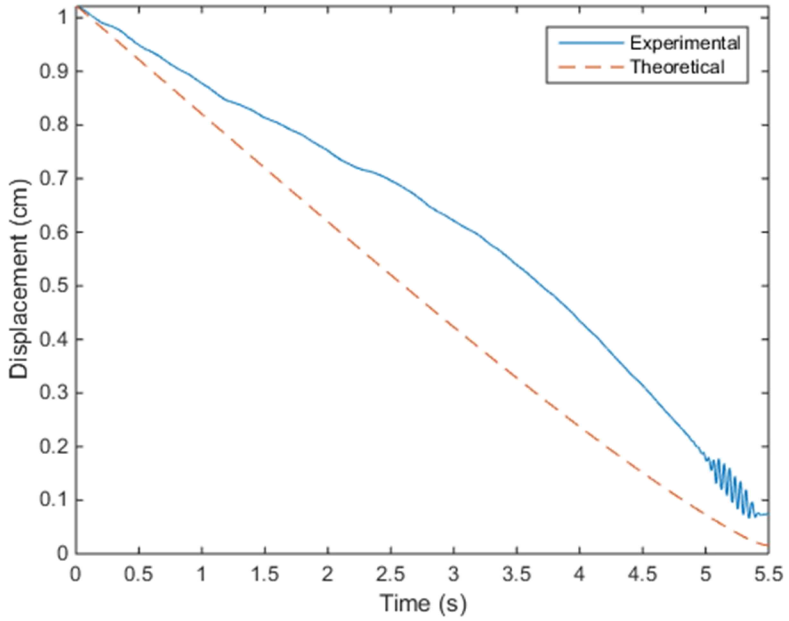

Figure 4.20: Case 9 Displacement Comparison

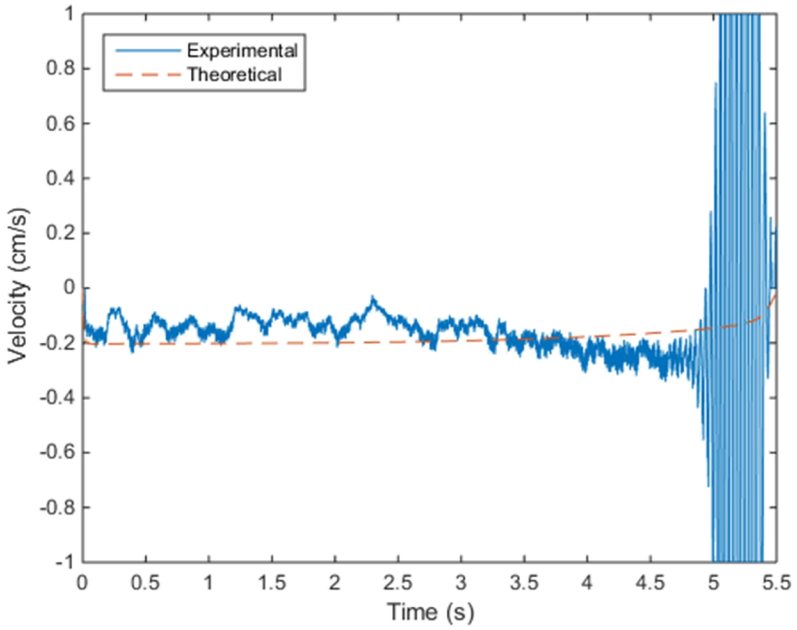

Figure 4.21: Case 9 Velocity Comparison

Students should see that there is a problem with assuming no friction or damping. The problem is that small values of u give a deadband and non-linear behavior seen in Figures 4.4-

4.9. Larger values of u give better behavior, however, the motor begins to saturate, as seen in Figures 4.18-4.21.

5. LINEAR QUADRATIC GAUSSIAN WITH LOOP TRANSFER RECOVERY

5.1 Experiment Goals

The main goal of this laboratory is to implement a Linear Quadratic Gaussian (LQG) controller. Students should be able to implement a state feedback controller on the ECP hardware and apply the Loop Transfer Recovery (LTR) method to tune the estimator so that the LQG design better approximates the Linear Quadratic Regulator (LQR). Students will then compare time responses of the actual and estimated states of the hardware response.

5.2 Experimental Procedure

The experiment again involves using the ECP210, shown in Figure 1.1, this time configured in a two degree of freedom set up as represented below in Figure 5.1.

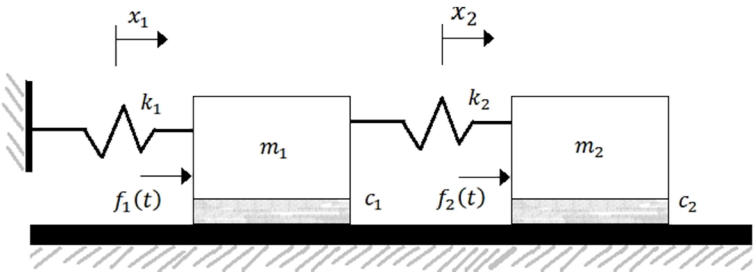

Figure 5.1: Model of the two degree of freedom system

In Figure 5.1, m_1 is the total mass of the first cart, m_2 is the total mass of the second cart, k_1 is the spring constant of the light spring, k_2 is the spring constant of the stiff spring, c_1 is the viscous damping constant of the first cart, c_2 is the viscous damping constant of the second cart, x_1 is the displacement of the first cart and x_2 is the displacement of the second cart. It should be

remembered that the inputs $f_1(t)$ and $f_2(t)$ are not what is specified in the Simulink block and should be rewritten by way of (5.1) and (5.2)

$$f_1(t) = C_{hw_1} g_1(t) \tag{5.1}$$
$$f_2(t) = C_{hw_2} g_2(t) \tag{5.2}$$

After the equations of motion have been found for the system, a choice of the system parameters should be made from the various cases from Chapter 1. Following this the system should be represented in state-space form as a system of n states, p inputs and q outputs such that:

$$\dot{\mathbf{x}} = \mathbf{A}\mathbf{x} + \mathbf{B}\mathbf{u} + \mathbf{L}\mathbf{v} \tag{5.3}$$
$$\mathbf{y} = \mathbf{C}\mathbf{x} + \mathbf{w} \tag{5.4}$$

and the state estimate equations are

$$\dot{\hat{\mathbf{x}}} = \mathbf{A}\hat{\mathbf{x}} + \mathbf{B}\mathbf{u} + \mathbf{H}_{kf}(\mathbf{y} - \hat{\mathbf{y}}) \tag{5.5}$$
$$\hat{\mathbf{y}} = \mathbf{C}\hat{\mathbf{x}} \tag{5.6}$$

where **L** is the process noise matrix and has dimensions $n \times p$, v is additive white Gaussian process noise, **w** is additive Gaussian measurement noise, $\hat{\mathbf{x}}$ is the estimate of the state, $\mathbf{H}_{kf}$ is the Kalman gain, $\hat{\mathbf{y}}$ is the estimate of the output and $\dot{\hat{\mathbf{x}}}$ is the first time derivative of the estimate of the state. After the system is set up, the controller gain and Kalman gain are to be calculated using the control algebraic Riccati equation and the filter algebraic Riccati equation, respectively. Students should then apply the LTR method to tune the estimator to better mimic the LQR's performance. A singular value plot overlaying the LQR's singular values with the singular values of the LQG and the various iterations of the LTR should be formed to illustrate the loop shaping of the LTR method. Then, as before, a pre-filter gain should be applied to the reference input to control the steady-state error to the applied step input [9]. The students should run the

unaltered LQG on the hardware, shown in Figure 5.2, and then implement iterations of the LTR method.

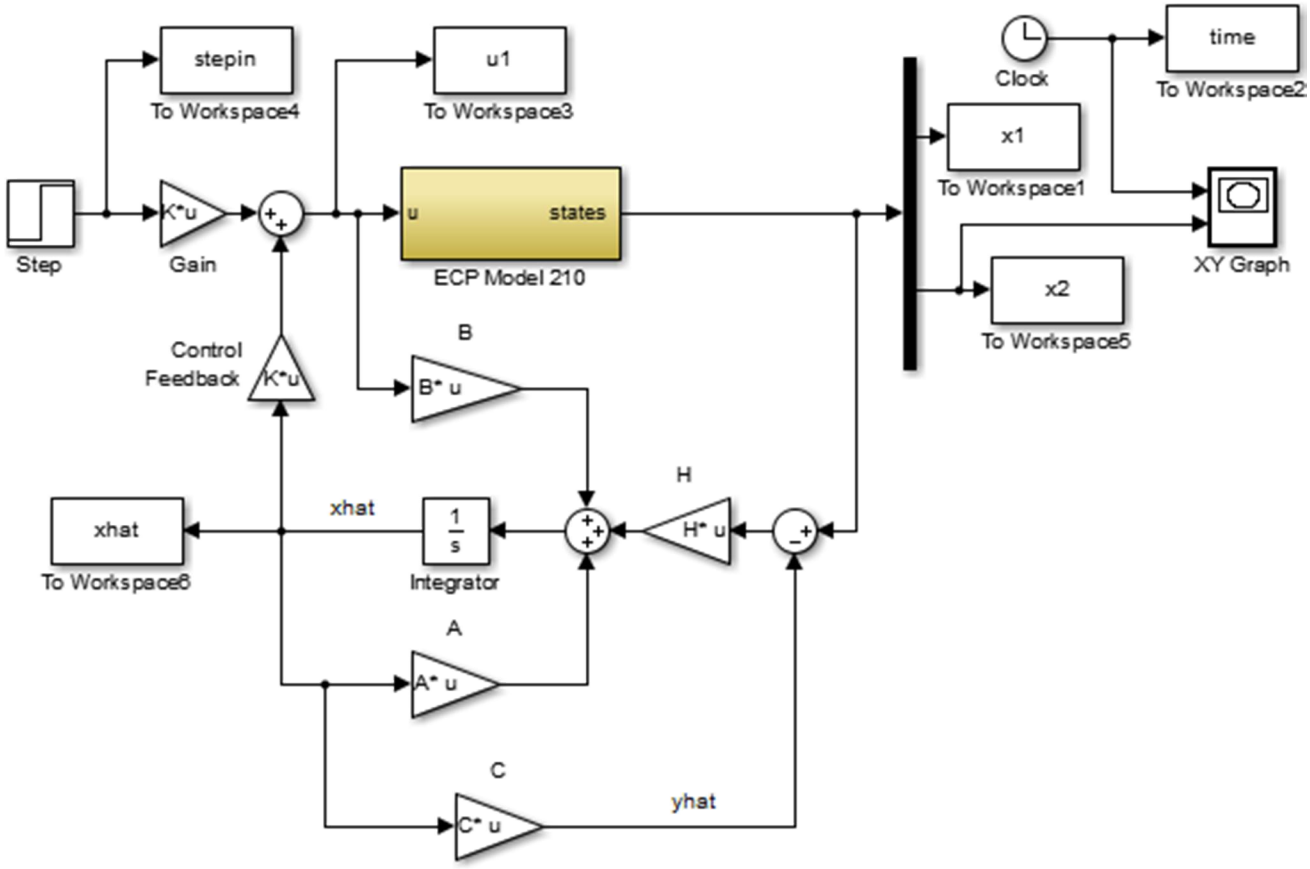

Figure 5.2: Simulink RTW

The plots of both the outputs and their estimates should then be compared from the various iterations of the LTR method.

5.3 Method of Analysis

To start calculations for the gains of the LQG, the controller gains shall be calculated first. To do this it is assumed that the controller is a perfect LQR and thus (5.3) and (5.4) become

$$\dot{\mathbf{x}} = \mathbf{Ax} + \mathbf{Bu} \tag{5.7}$$

$$\mathbf{y} = \mathbf{Cx} \tag{5.8}$$

Substituting the control law

$$\mathbf{u} = \mathbf{Kx} = -\mathbf{R}^{-1}\mathbf{B}^T\boldsymbol{\lambda} \tag{5.9}$$

into the new state equations and concatenating the state and costate equations, using a similar cost function as (4.6), to a $2n \times 2n$ can be obtained as

$$\begin{Bmatrix} \dot{\mathbf{x}} \\ \dot{\boldsymbol{\lambda}} \end{Bmatrix} = \begin{bmatrix} \mathbf{A} & -\mathbf{B}\mathbf{R}^{-1}\mathbf{B}^T \\ -\mathbf{Q} & -\mathbf{A}^T \end{bmatrix} \begin{Bmatrix} \mathbf{x} \\ \boldsymbol{\lambda} \end{Bmatrix} \tag{5.10}$$

where $\mathbf{Q}$ is a symmetric positive semidefinite real constant matrix and $\mathbf{R}$ is a symmetric positive definite real constant matrix. The control law (5.9) implies that $\mathbf{x}$ and $\boldsymbol{\lambda}$ are related by a transformation $\mathbf{P}$ such that

$$\lambda = \mathbf{P}\mathrm{x} \tag{5.11}$$

or

$$\mathbf{Kx} = -\mathbf{B}\mathbf{R}^{-1}\mathbf{Px} \tag{5.12}$$

By the product rule, the time derivative of $\boldsymbol{\lambda}$ is

$$\dot{\boldsymbol{\lambda}} = \dot{\mathbf{P}}\mathbf{x} + \mathbf{P}\dot{\mathbf{x}} \tag{5.13}$$

Substituting this into the costate equation,

$$\dot{\mathbf{P}}\mathbf{x} + \mathbf{P}\dot{\mathbf{x}} = -\mathbf{Q}\mathbf{x} - \mathbf{A}^T\boldsymbol{\lambda} \tag{5.14}$$

Substituting the state equation for $\dot{\mathbf{x}}$ into (5.14),

$$\dot{\mathbf{P}}\mathbf{x} + \mathbf{P}(\mathbf{A}\mathbf{x} - \mathbf{B}\mathbf{R}^{-1}\mathbf{B}^T\boldsymbol{\lambda}) = -\mathbf{Q}\mathbf{x} - \mathbf{A}^T\boldsymbol{\lambda} \tag{5.15}$$

Inserting (5.11) into (5.15),

$$\dot{\mathbf{P}}\mathbf{x} + \mathbf{P}(\mathbf{A}\mathbf{x} - \mathbf{B}\mathbf{R}^{-1}\mathbf{B}^T\mathbf{P}\mathbf{x}) = -\mathbf{Q}\mathbf{x} - \mathbf{A}^T\mathbf{P}\mathbf{x} \tag{5.16}$$

Collecting terms,

$$\dot{\mathbf{P}}\mathbf{x} + (\mathbf{P}\mathbf{A} - \mathbf{P}\mathbf{B}\mathbf{R}^{-1}\mathbf{B}^T\mathbf{P} + \mathbf{Q} + \mathbf{A}^T\mathbf{P})\mathbf{x} = \mathbf{0} \tag{5.17}$$

assuming steady state and since it is desired to find $\mathbf{P}$ for any $\mathbf{x}$

$$(\mathbf{P}\mathbf{A} - \mathbf{P}\mathbf{B}\mathbf{R}^{-1}\mathbf{B}^T\mathbf{P} + \mathbf{Q} + \mathbf{A}^T\mathbf{P}) = \mathbf{0} \tag{5.18}$$

This is the Control Algebraic Riccati Equation (CARE) solving for $\mathbf{P}$, $\mathbf{K}$ can be found from (5.12).

Once the controller gain is determined the Kalman gain should be determined. The first step in this is choosing an arbitrary positive definite matrix $\mathbf{W}$ such that $\mathbf{W} > \mathbf{0}$ and $\mathbf{W}^{-1}$ exists. $\mathbf{L}$ is given such that $[\mathbf{A}, \mathbf{L}]$ is stabilizable, that is if all unstable modes are controllable. Let

$$\mathbf{\Xi} = \mathbf{L}\mathbf{L}^T \tag{5.19}$$

then the Filter Algebraic Riccati Equation (FARE) should be solved.

$$\mathbf{A}\mathbf{\Sigma} + \mathbf{\Sigma}\mathbf{A}^T + \mathbf{\Xi} - \mathbf{\Sigma}^T\mathbf{C}^T\mathbf{W}^{-1}\mathbf{C}\mathbf{\Sigma} = \mathbf{0} \tag{5.20}$$

where $\mathbf{\Sigma}$ is the solution of the FARE. The Kalman gain, which is the gain of the Kalman filter, is calculated from the FARE

$$\mathbf{H}_{kf} = \mathbf{\Sigma}\mathbf{C}^T\mathbf{W}^{-1} \tag{5.21}$$

The FARE has duality with the CARE as displayed in Table 5.1 [9].

Table 5.1: Duality Properties

FARE	CARE
$\mathbf{A}$	$\mathbf{A}^T$
$\mathbf{C}$	$\mathbf{B}^T$
$\mathbf{W}$	$\mathbf{R}$
$\mathbf{L}$	$\mathbf{Q}^{\frac{1}{2}}$
$\mathbf{\Sigma}$	$\mathbf{P}$
$\mathbf{H}$	$\mathbf{K}$
$(\mathbf{A}, \mathbf{C})$ detectable	$(\mathbf{A}, \mathbf{B})$ stabilizable
$(\mathbf{A}, \mathbf{L})$ stabilizable	$\left(\mathbf{A}, \mathbf{Q}^{\frac{1}{2}}\right)$ detectable

Once the LQG controller has been designed it is time to implement the LTR method. For this laboratory this is rather simple. It is necessary to set

$$\mathbf{Q} = \mathbf{C}^T\mathbf{C} \tag{5.22}$$

and

$$\mathbf{\Xi} = \mathbf{L}\mathbf{L}^T + q^2\mathbf{B}\mathbf{B}^T \tag{5.23}$$

where q is a scalar parameter. The Kalman gain should be recalculated with increasing values of q until the LQG is close to the LQR [9, 11, 12].

5.4 Sample Results

The parameters used for the development of this laboratory can be seen in Table 5.2

Table 5.2: Parameters Used

Cart	m_{ti} (kg)	c_i (Ns/m)	k_i (N/m)	C_{hw_i}
1	1.7869	7.1077	326.7	7394.5
2	2.06	7.4	741.2	6203.7

For the development of this laboratory **L** was chosen to be

$$\mathbf{L} = \begin{bmatrix} 31.472 & 31.472 \\ 40.579 & 40.579 \\ -37.301 & -37.301 \\ 41.338 & 41.338 \end{bmatrix} \tag{5.24}$$

and **w** as

$$\mathbf{W} = \begin{bmatrix} 1 & 0 \\ 0 & 1 \end{bmatrix} \tag{5.25}$$

Also **R**, was chosen as

$$\mathbf{R} = \begin{bmatrix} 7.5 & 0 \\ 0 & 7.5 \end{bmatrix} \tag{5.20}$$

The parameter q for each LTR system was chosen as

$$q = 10^{n/4} \tag{5.26}$$

for $n = 1, 2, 3, 4$. To develop the control gain, **Q** was selected as

$$\mathbf{Q} = \mathbf{G}^T\mathbf{G} \tag{5.27}$$

where

$$\mathbf{G} = \begin{bmatrix} 0 & 0.2 & 1 & 0 \\ 0 & 0.2 & 1 & 0 \end{bmatrix} \tag{5.28}$$

With this information **K** is found from (5.12)

$$\mathbf{K} = \begin{bmatrix} -0.0137 & 0.0086 & 0.364 & 0.0041 \\ -0.0149 & 0.003 & 0.3511 & 0.0136 \end{bmatrix} \tag{5.29}$$

The Kalman gains for each case can be seen in Table 5.3

Table 5.3: Kalman Gain for each case

LQG	$n = 1$	$n = 2$	$n = 3$	$n = 4$
$\begin{bmatrix} 33.83 & -28.51 \\ -11.50 & 273.77 \\ -28.51 & 38.68 \\ 6.42 & -236.8 \end{bmatrix}$	$\begin{bmatrix} 120.7 & -68 \\ 632 & 444.5 \\ 68 & 109.5 \\ 329.1 & 4.629 \end{bmatrix}$	$\begin{bmatrix} 160 & -5 \\ 11872 & 460 \\ -5 & 142 \\ 329 & 8672 \end{bmatrix}$	$\begin{bmatrix} 213 & -4 \\ 21815 & 496 \\ -4 & 186 \\ 328 & 15919 \end{bmatrix}$	$\begin{bmatrix} 285 & -3 \\ 39614 & 457 \\ -3 & 246 \\ 325 & 28892 \end{bmatrix}$

This leads to the singular values plot seen in Figure 5.3

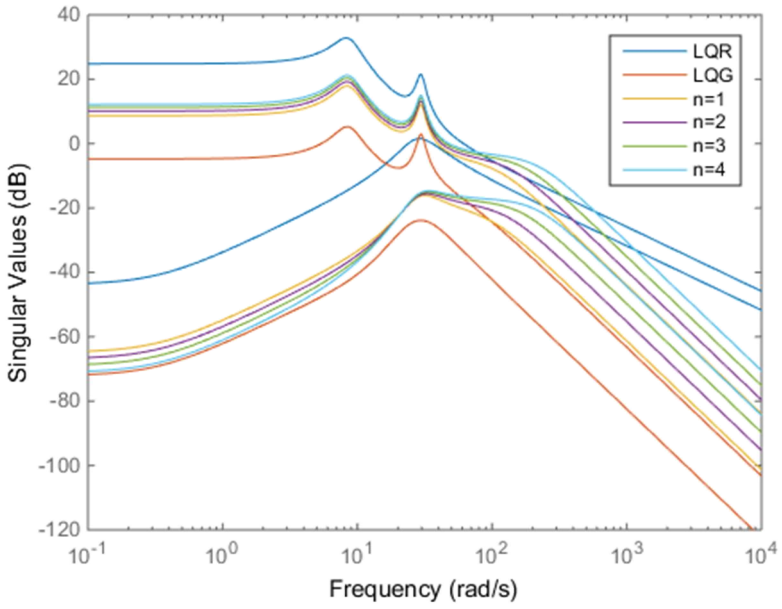

Figure 5.3: Singular values of the systems to be compared

Students should see from the singular values plot that increasing q will lead to better approximations of the LQR.

Plots comparing the measured states with their estimates can be seen in Figures 5.4-5.13

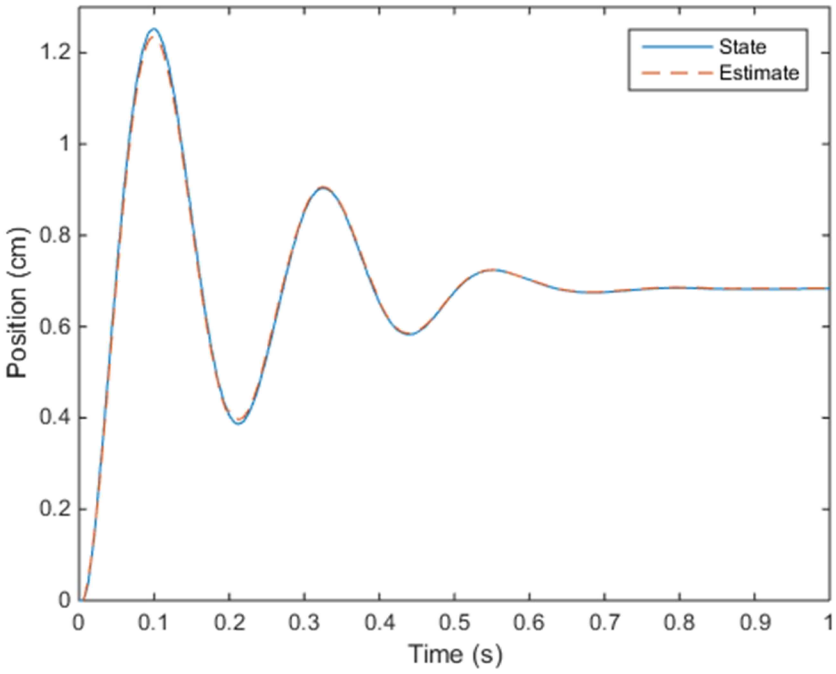

Figure 5.4: LQG first cart position with its estimate

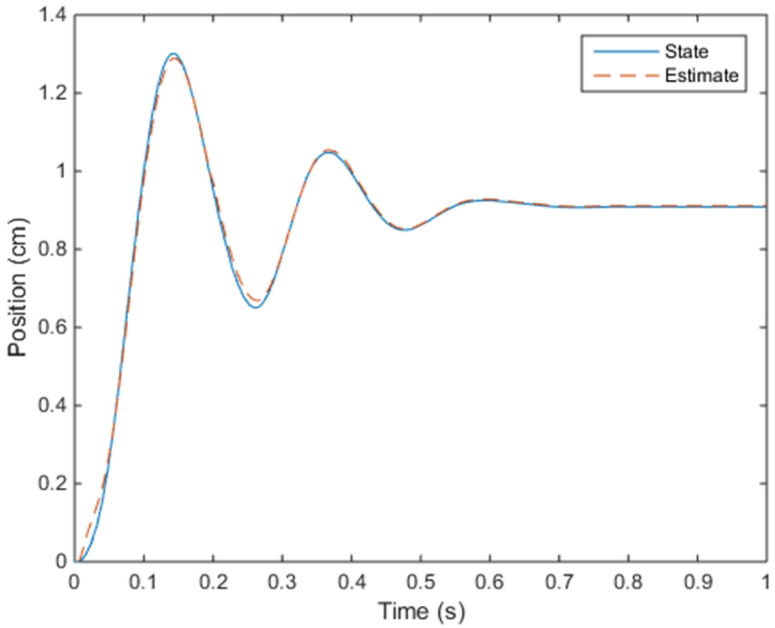

Figure 5.5: LQG second cart position with its estimate

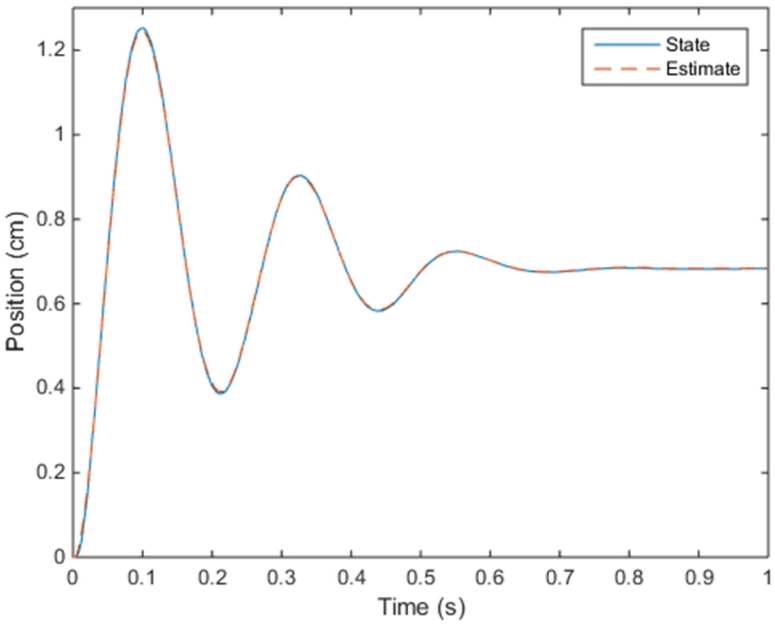

Figure 5.6: First cart position with its estimate for $n = 1$

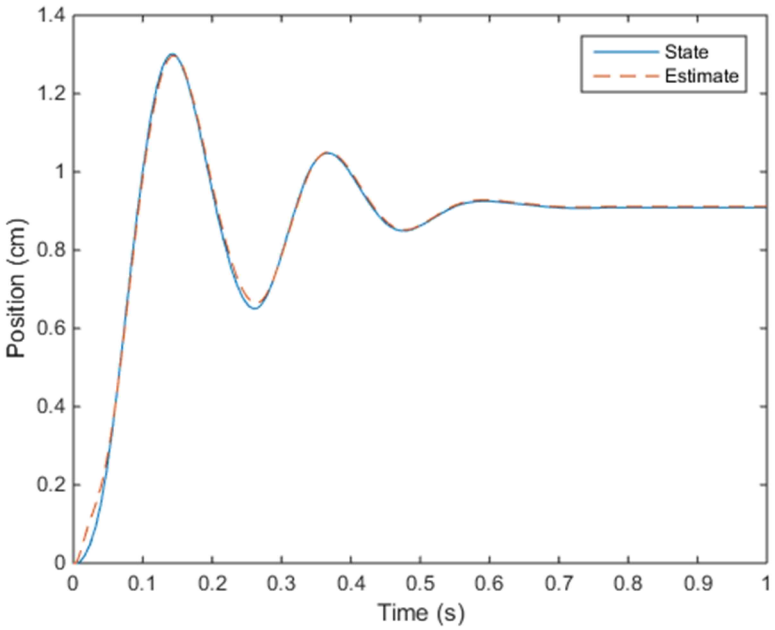

Figure 5.7: Second cart position with its estimate for $n = 1$

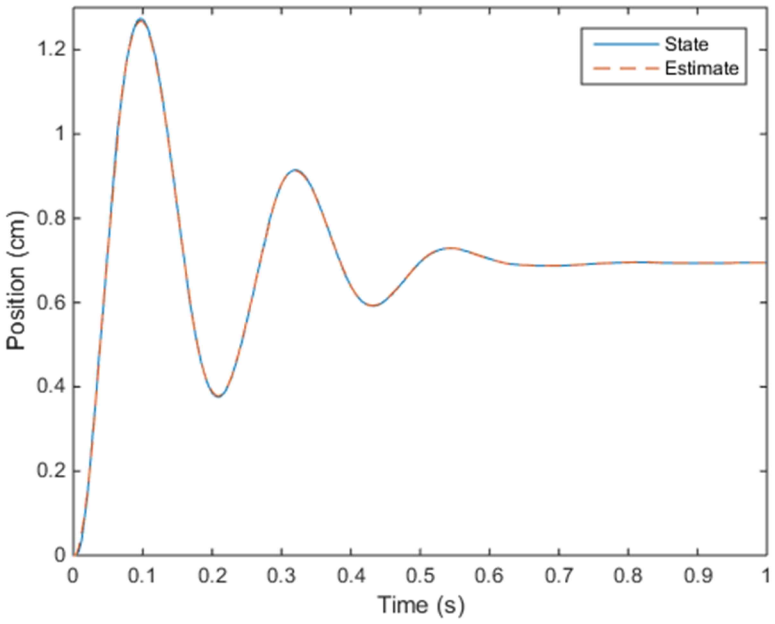

Figure 5.8: First cart position with its estimate for $n = 2$

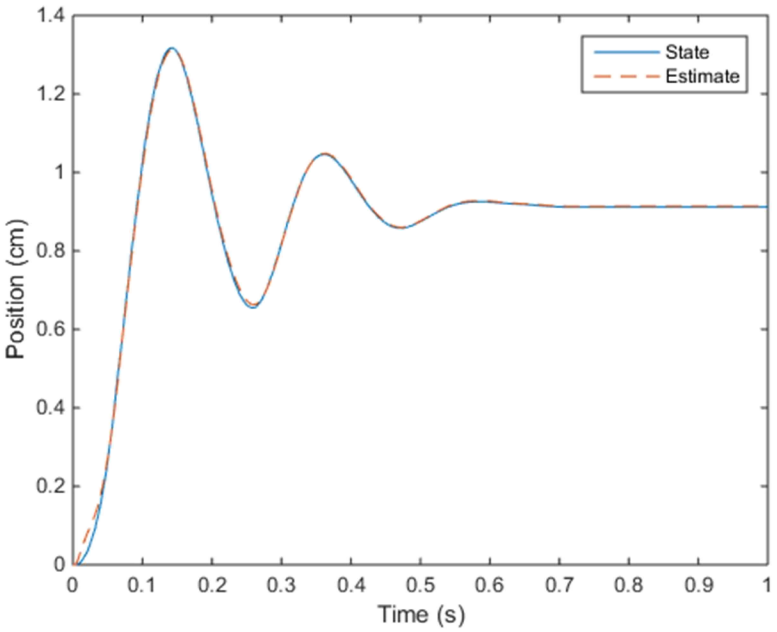

Figure 5.9:Second cart position with its estimate for $n = 2$

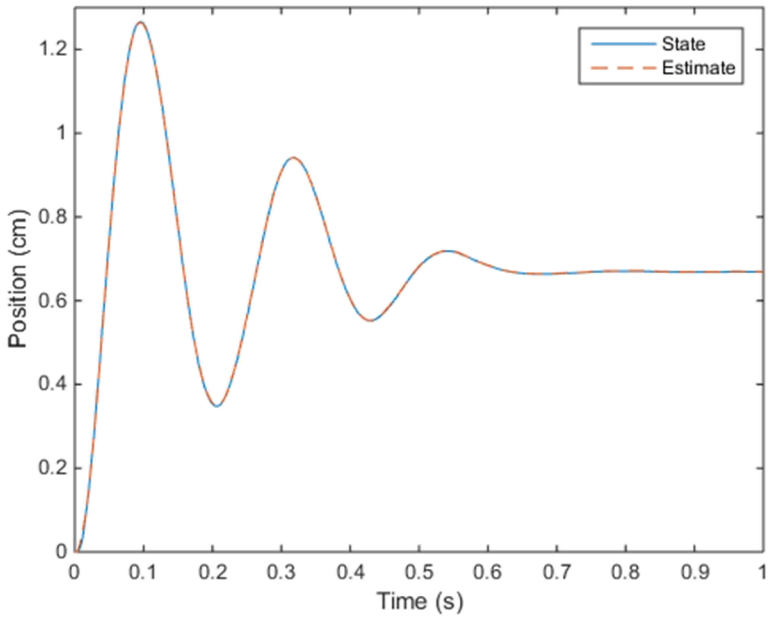

Figure 5.10: First cart position with its estimate for $n = 3$

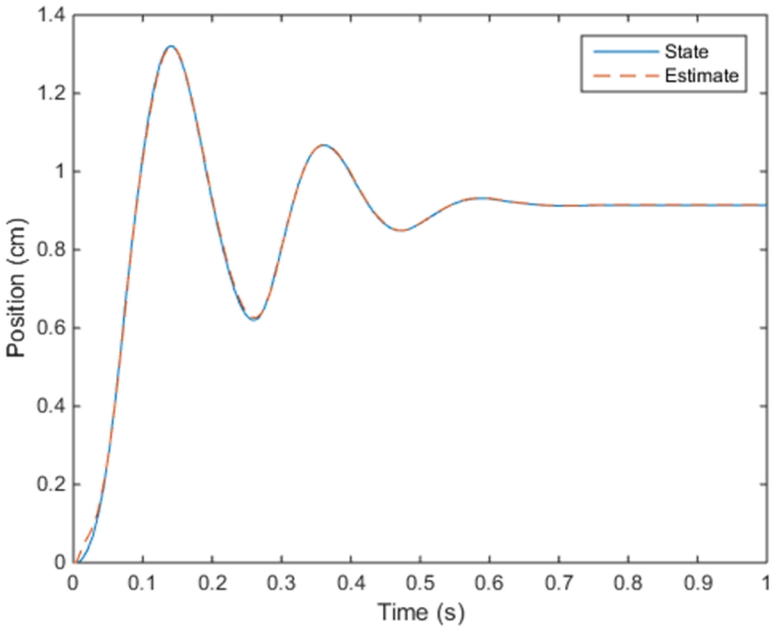

Figure 5.11:Second cart position with its estimate for $n = 3$

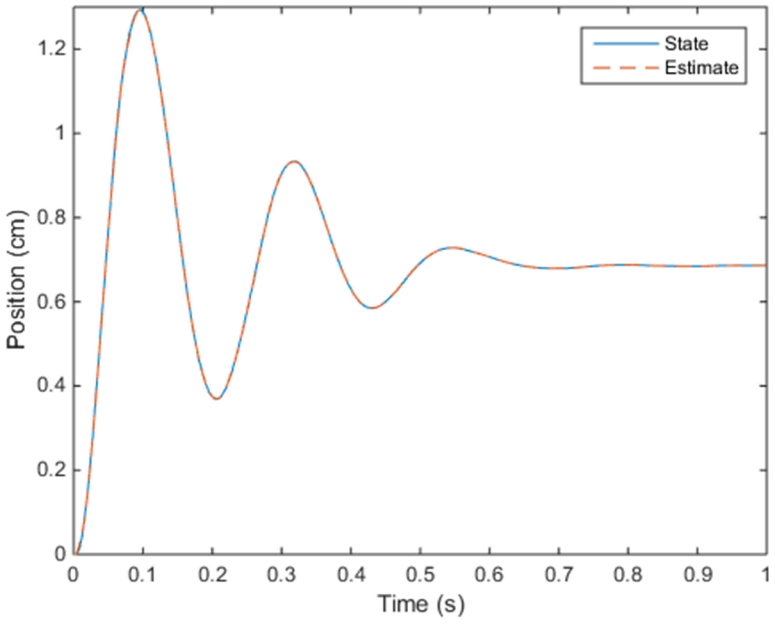

Figure 5.12: First cart position with its estimate $n = 4$

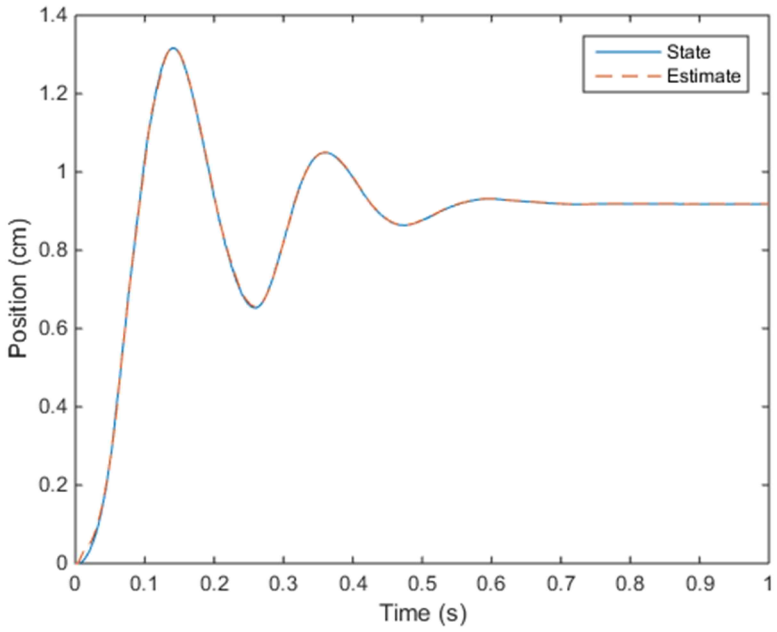

Figure 5.13: Second cart position with its estimate $n = 4$

Students should note that higher q leads to better estimates especially in the estimate of the second cart.

6. Conclusion and Future Work

6.1 Conclusion

A series of advanced control laboratories has been developed and demonstrated for educational purposes in advanced controls courses. The learning objectives as well as the control techniques of each laboratory have been spelled out and demonstrated. Students should realize the problems that arise from using a linear model, and the limitations of what can be done with hardware when compared to what can be done mathematically. However, the overall goal of this laboratory series is to provide students with hands on hardware in the loop laboratories using advanced control techniques. This environment was adapted from existing equipment, required no new purchases and showed the viability of using advanced control techniques on the ECP210 despite it not being designed to do so. The primary challenge of developing this lab series was the difference in the strength of the disturbance motor compared to the primary motor of the ECP210. This was especially true of the MIMO parts of the laboratory series where the motors were interacting with each other.

6.1 Future Work

A natural extension of the work presented is its actual implementation in an educational environment. This should be paired with post-course student surveys to see if the students' knowledge and confidence on the topics were significantly increased. Additionally more control

topics could be added to eventually justify a dedicated laboratory credit. These topics could include Nyquist design criteria, LQR control, and H_∞ control.

LIST OF REFERENCES

[1] Feisel, Lyle D., and Albert J. Rosa. "The Role Of The Laboratory In Undergraduate Engineering Education." *Journal Of Engineering Education* 94.1 (2005): 121-130. Academic Search Premier. Web. 30 Sep. 2013.

[2] Roemer, R.B.; Setbacken, Robert M., "A Design Oriented Feedback Control Laboratory," *Education, IEEE Transactions on,* vol.22, no.3, pp.145,147, Aug. 1979

[3] Precup, R.; Preitl, S.; Radac, M.; Petriu, E.M.; Dragos, C.; Tar, J.K., "Experiment-Based Teaching in Advanced Control Engineering," *Education, IEEE Transactions on*, vol.54, no.3, pp.345,355, Aug. 2011

[4] Howe, R. M., "Analog Computers in Academia and Industry," *IEEE Contr. Syst. Mag.*, vol. 25, no. 3, pp.37-43, June 2005.

[5] Spiess, R., "The Comdyna GP-6 Analog Computer," *IEEE Contr. Syst. Mag.*, vol. 25, no. 3, pp.68-73, June 2005.

[6] "Educational Control Products - Dynamics and Vibrations - Rectilinear Plant." *Educational Control Products - Dynamics and Vibrations - Rectilinear Plant*. Web. 18 October 2014. <http://www.ecpsystems.com/controls_recplant.htm>

[7] Burchett, Bradley T. *Dynamic Modeling and Simulation*. 1st ed. N.p.: Bradley T. Burchett, 2011.

[8] Andry, A.N.; Shapiro, E.Y.; Chung, J.C., "Eigenstructure Assignment for Linear Systems," *Aerospace and Electronic Systems, IEEE Transactions on,* vol.AES-19, no.5, pp.711,729, Sept. 1983

[9] Franklin, Gene F., J. D. Powell, and Abbas Emami-Naeini. *Feedback Control of Dynamic Systems*. 5th ed. Saddle River: Pearson Prentice Hall, 2006. Print.

[10] Burchett, B. T., "Euler–Lagrange Optimal Control for Symmetric Projectiles", *Proceedings of the AIAA Science and Technology Forum and Exposition 2015*, Kissimee, FL, 5-9 January, 2015.

[11] Stein, G.; Athans, M., "The LQG/LTR procedure for multivariable feedback control design," *Automatic Control, IEEE Transactions on* , vol.32, no.2, pp.105,114, Feb 1987

[12] Doyle, J.; Stein, G., "Multivariable feedback design: Concepts for a classical/modern synthesis," *Automatic Control, IEEE Transactions on* , vol.26, no.1, pp.4,16, Feb 1981

APENDIX A

The findmag2 used in analyzing the frequency response data:

```
function [Magx] = findmag2(x,u)
%
% utility to find the magnitude from freq resp data:
%
% [Magx] = findmag2(x,u)
%
% Determines the Bode magnitude ratio from a set of frequency response data
% x = response of first mass
% u = amplitude of input
%
% Assumes that the data set is 5000 samples long
% (Equivalent to 20s of ECP data under RTW)
n = 500;
p1 = polyfit(1:(n+1),x(end-n:end)',1);

Enc1cm = x(end-n:end) - (polyval(p1,1:(n+1)))';

Magx = max(Enc1cm)/u;
```